Scacchi, A.; Vuorte, M.; Sammalkorpi, M.

Multiscale modelling of biopolymers

Published in:
Advances in Physics: X

DOI:
10.1080/23746149.2024.2358196

Published: 03/07/2024

Document Version
Publisher's PDF, also known as Version of record

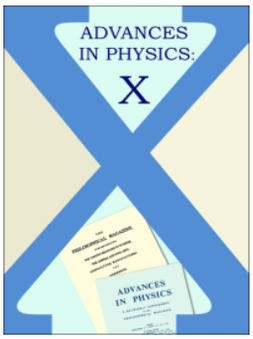

Advances in Physics: X

ISSN: (Print) (Online) Journal homepage: www.tandfonline.com/journals/tapx20

Multiscale modelling of biopolymers

A. Scacchi, M. Vuorte & M. Sammalkorpi

To cite this article: A. Scacchi, M. Vuorte & M. Sammalkorpi (2024) Multiscale modelling of biopolymers, Advances in Physics: X, 9:1, 2358196, DOI: 10.1080/23746149.2024.2358196

To link to this article: https://doi.org/10.1080/23746149.2024.2358196

Published online: 03 Jul 2024.

ADVANCES IN PHYSICS: X
2024, VOL. 9, NO. 01, 1–55
https://doi.org/10.1080/23746149.2024.2358196

Taylor & Francis
Taylor & Francis Group

REVIEWS

Multiscale modelling of biopolymers

A. Scacchi[a,b,c,d], M. Vuorte[c,e] and M. Sammalkorpi[b,c,e]

[a]Department of Applied Physics, Aalto University, Aalto, Finland; [b]Department of Bioproducts and Biosystems, Aalto University, Aalto, Finland; [c]Academy of Finland Center of Excellence in Life-Inspired Hybrid Materials (LIBER), Aalto University, Aalto, Finland; [d]Department of Mechanical and Materials Engineering, University of Turku, Turku, Finland; [e]Department of Chemistry and Materials Science, Aalto University, Aalto, Finland

ABSTRACT

This review overviews common biopolymer modelling approaches ranging from chemically specific to highly coarse-grained techniques, along with their application ranges, strengths and limitations. Recent modelling applications at each modelling scale are outlined and discussed. The focus is on modelling of protein and peptide, nucleic acid and saccharide-based biopolymer systems, excluding lignocellulose materials. The survey focuses on physics-based models. We cover particle-based simulations methods, including all-atom and coarse-grained molecular dynamics (MD), dissipative particle dynamics (DPD) and Langevin and Brownian dynamics (BD) approaches. While these methods capture molecular and particle-level dynamics, a brief overview of also stochastic sampling approaches (Monte Carlo methods) to physics-based models, as well as free energy functional-based methods, i.e. field theory approaches, such as self-consistent field theory (SCFT) and classical density functional theory (cDFT), are provided.

ARTICLE HISTORY
Received 13 February 2023
Accepted 17 May 2024

KEYWORDS
Biopolymer modelling; physics-based models; polymer materials modelling

CONTACT A. Scacchi alberto.scacchi@utu.fi Department of Mechanical and Materials Engineering, University of Turku, Turku FI-20014, Finland; M. Sammalkorpi maria.sammalkorpi@aalto.fi Department of Chemistry and Materials Science, Aalto University, Aalto FI-00076, Finland

GRAPHICAL ABSTRACT

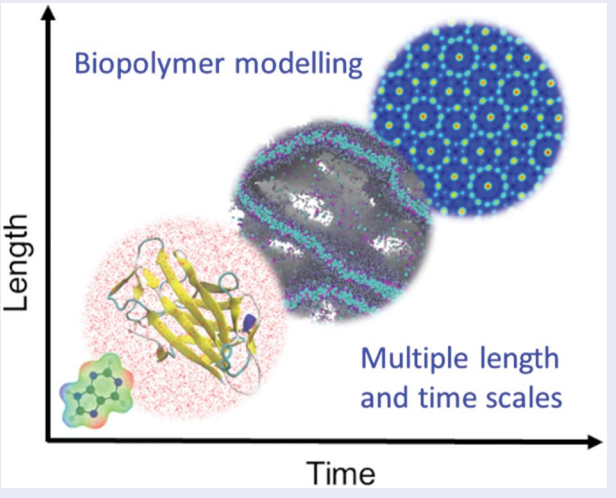

1. Introduction

The term *biopolymer* refers to a polymer whose constituents are based on living matter; biopolymers themselves or their synthesis requisites originate from nature [1,2]. Biopolymers include homo- or heteropolymers of nucleic acids, amino acids or saccharides. Examples include, e.g., DNA and RNA, proteins composed of amino acids, and various polysaccharides, such as cellulose, and at more general level, lignocellulosic biomass [2,3]. Furthermore, polymers synthesised in vitro from biological sources, e.g. bio mass, bio oils, animal fats, sugars, proteins, and amino acids may also be classified as biopolymers [2,4]. Polyesters are a very well-known example [2,4,5]. Worth noting is that the term 'biopolymer' sometimes refers to also polymers that can be bio-based but not biodegradable (e.g. bio-based polyethylene), as well as, biodegradable polymers produced from fossil fuel-based sources (e.g. poly(ε-caprolactone)) [2,6]. Here, we use the term biopolymers for polymers that are from nature, meaning that either the polymers themselves or their monomeric components originate from nature.

In nature, biopolymers have functions that are often highly specific, sometimes complex, and tightly connected with their properties [1,2]. Their functions relate to, e.g., conservation and expression of genetic information, storage of carbon and energy in chemical bonds, catalysis of chemical reactions, mediation of intracellular communication, as well as communication and interaction between a living cell and its surrounding. Biopolymers also play a crucial role in biomechanics and biological materials [7]. In materials science, and as materials solutions, biopolymers, especially biobased

plastics, offer very timely and interesting sustainable and biodegradable alternatives to synthetic plastics [8,9]. Notably, synthetic plastics, ubiquitous in their use [10], have concerning effects on ecosystems, especially on marine life [11], but also weight in carbon emissions [12]. As a drastic increase of production and use of them in the coming decades is predicted [13,14], finding more sustainable and biodegradable substitutes is becoming increasingly important [9]. Biopolymers hold significant promise in this [8,9].

Besides sustainability, biopolymers and biopolymer-based composites have advantage in technological applications because of many of them being cheap, naturally abundant, and easily functionalized to tunable properties via surface chemistry and functionality [2,6]. For example, air and water filtration [15], packaging materials [16–19], and food preservation solutions [20,21] benefit in properties by being biopolymer-based. Biopolymers also find abundant use in bioengineering applications, such as bioadhesives [22], medical devices, and bioengineering interfaces materials, as well as, in tissue engineering [23–26].

Especially abundant in technological applications are polyester-based materials and polyester composites, see e.g. Refs. [4,5] for recent reviews. Polyesters can compose both durable and biodegradable plastics, and their properties can be readily modified by suitable polymer design and modifications [4]. Polyesters offer a number of high technological applications, such as materials for energy conversion devices, shielding composite materials for electromagnetic fields, bioengineering applications, but also materials with performance superior to Kevlar, and elevated storage modulus and viscoelastic stiffness [5]. Therefore, it is not surprising that most biobased polymers produced for applications are polyesters [4]. Also other biopolymers form interesting basis for composites, see e.g. Refs. [2,4,6]: a novel direction, with promising functionalities, due to the self-assembly properties rising from secondary structure, are protein-based (composite) biomaterials that are degradable, biocompatible, and offer increased tunability via the amino acids and secondary structure [27]. Peptide and protein-based materials present pioneering solutions in the fields of nanoreactors, sensors, electronics, and responsive materials to external stimuli [28]. Peptide- and protein-nanoparticle conjugates offer advanced materials for treatment, diagnosis, and prevention of diseases [29].

Biopolymers can either be extracted from their natural chassis species, collected as an extracellular product, be synthesized *in vivo* or produced from renewable biomass feedstocks [30]. Production means, and resulting properties, are reviewed in Refs. [2,4]. As a novel direction, an increasing interest in biosynthetic *in vivo* production exists [4,31,32]. Current biopolymer research has focused mostly on improving the inherently poor mechanical properties, fatigue issues (short life time), low chemical resistance, poor long-term durability, and limited processing capability of naturally occurring biopolymers,

as well as, on introducing additional functionality [33–37]. However, the underlying hierarchical multiscale dependency of materials properties and response make advanced knowledge guided design of polymeric materials challenging [38,39].

Computational and theoretical models offer a versatile tool for designing, predicting, understanding, and optimizing structure and properties of biopolymer-based systems, as well as extracting multiscale dependencies characteristics [39]. For biopolymer materials and biological processes, the typical length scales span from a single chemical bond at the ångström scale, to interactions at monomer and individual polymer chain level, but also to the domain formation and higher degree three-dimensional structure formation that is characteristic to these systems [39,40]. Traditionally, this μm and mm range structural order rises, e.g., in crystallization domains and in mixing characteristics of polymer blends and composites [41]. For biopolymers, additional contributions to structure formation rise from the hierarchical higher order assembly structures of, e.g., proteins and polysaccharides [2]. Naturally, for (bio)polymer systems, also the continuum scale is relevant [40]. Similarly, also the time scales of the dynamics of interest span from the fs range of chemical bond formation and breaking, to hours, corresponding to phenomena such as large scale phase separation and protein aging, involving secondary and tertiary structure changes in crowded environments [39]. For polymeric systems, the relevant phenomena thus occur at such wide temporal and spatial resolution landscape that a single theory or computational approach does not cover everything, consequently requiring approaches at multiple scales [41].

In this review, we give an overview on common (non-quantum mechanical) biopolymer modelling methods, ranging from microscopic to field theory levels, covering both the atomistic detail level phenomena and macroscopic approaches. Although not at the focus of this review, quantum mechanics (QM)-based modelling methods are well-suited for studying biopolymer-related systems of few hundreds to thousands of atoms in detail, including the energetics and dynamics of chemical reactions and exploration of conformer space and spectroscopic properties. Depending on the level of theory, extent of extrapolation, and amount of computational resources, QM methods may be used, at one end, to provide detailed potential energy surface and spectroscopic behaviour of, e.g., individual amino acids [42–45], and, at the other end, to predict folding patterns of protein domains [46–48]. Combined with classical simulations approaches, QM methods are also used for examining the energetics and dynamics of biomolecule – ligand interactions [49–51]. QM methods can produce high-quality reference data, such as spectroscopic data on molecules in gas phase without complicating interactions from the environment; such data is used, e.g., to complement and guide experiments, as well as in parametrization and development of bottom-up

semi-classical and classical modelling approaches [52,53]. Recent developments of QM-based methods for biomolecular simulations are reviewed in Refs. [49,54–58].

Although data-based methods are becoming more significant for materials science [59,60], we limit the review to physics-based models. While the emphasis is on the methods at basic level, we also showcase some recent examples of research, demonstrating modelling reachable by the approaches. We focus the examples in the direction of biopolymer based materials, however largely excluding cellulose and polyester modelling literature, as both cellulose and polyester-based materials have such high technological relevance that they attract numerous reviews. For example, the direction of modelling in lignocellulose-based materials has been recently reviewed several times [61–64]. Polyesters modelling is discussed in Refs. [65,66].

2. Computational approaches to biopolymer materials modelling

Classical computational materials modelling methods can generally be categorized into particle-based, field-based, and continuum modelling approaches. Appropriately named, particle-based models represent the polymer at resolution of individual atoms, chemical groups, monomers, or even regions of a polymer melt or solution, by particles [67]. The particles interact according to effective potentials that model the dominant physicochemical interactions for capturing the response at each description length and time scales [67]. Sampling of the possible states in the particle system typically follows a specified thermodynamic ensemble, and the system has either deterministic or stochastic dynamics, from which (non-)equilibrium energetics of the process of interest, as well as the associated structural and mechanical characteristics, can be extracted [67,68]. By contrast, field-based approaches typically describe the system of interest in terms of energy functionals, effective potentials, density fields, and collective dynamic variables, providing materials scale description [69]. Once again, both equilibrium and time-dependent properties of the material can be obtained. Continuum modelling approaches correspond to the numerical implementations rising from classical continuum mechanics considerations.

Another way to classify modelling approaches is to consider the accessible length and time scales, as depicted in Figure 1. For events occurring at atomistic scale, or related to electronic structure, such as chemical bond formation, electronic excitations and, e.g., electrochemical phenomena, QM methods capture the response. However, the high computational cost limits the modelling to some thousands of atoms, and such time scales of the dynamics that the modelling approaches remain limited in biopolymer modelling. Regardless, QM approaches are broadly used in biopolymer-related systems, and extensive reviews exist, e.g. in the context of proteins [70–72], peptides [71],

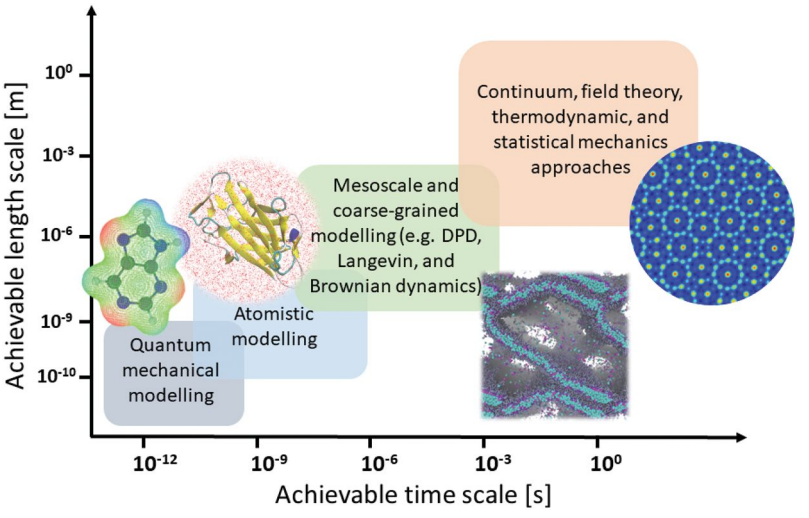

Figure 1. Different modelling approaches and their corresponding achievable time and length scales.

nucleic acids [72], and more generally for biological systems [73,74]. We focus here on larger scale approaches. A more relevant, yet still extremely limited (typically up to $(30\ \text{nm})^3$ in size; up to μs in time modelling approach in the biopolymer context is atomistic detail MD [67]. Benchmark simulations with up to a billion atoms for up to 100 ns simulation time exist, which use MD simulation codes with highly optimized calculation of non-bonded interactions and high level of parallelization [75–77]. At atomistic MD modelling extent of detail, structural and dynamical information at the level of atoms, chemical groups, and short polymers (oligomers) interactions, both in melts and in solutions, can be obtained. MD has in recent years become a hugely popular research tool, see Section 3. However, microphase separation and higher order structure formation are not captured due to limiting length and time scales. For these, different level of coarse-grained (CG) and mesoscale modelling approaches are needed. While capturing length and time scales in biopolymer assembly up to mm lengths and from tens of μs to ms (depending on the level of coarse-graining), these approaches loose, to a varying degree, the chemical specificity of the biopolymers. For example, atomistic detail structural features, such as localized charge correlations and hydrogen bonding, but also solvent-specific effects rising from such microstructure, are typically lost by coarse-graining. However, these methods are powerful in capturing, e.g., assembly response due to miscibility differences and large-scale structural organization that is independent of microscopic detail. Non-localized characteristics, such as, hydrophobicity, hydrophilicity, and solvation differences, are captured efficiently by CG approaches, see

Sections 3-5. While the majority of common particle-based modelling approaches of biopolymers capture dynamics evolution, in Section 6 we touch on stochastic sampling approaches to particle-based modelling. Considering the microscopic detail character only as mean or effective overall influence, field-based statistical mechanics and continuum level approaches capture large-scale materials response. These approaches are not subject to similar challenges in achievable length and time scale as particle-based methods, see Section 7.

3. Molecular dynamics for modelling of biopolymers

Although atomistic detail modelling of biopolymers can count on various sampling and dynamics choices, from, e.g., energy minimization approaches, docking, and various stochastic sampling approaches, the most common choice in examining structure, assembly and dynamics at this level relies on MD [68,78]. MD is a numerical method for obtaining the equilibrium and transport properties of a system of particles based on the integration of Newton's equations of motion

$$m_i \frac{d\mathbf{v}_i(\mathbf{r}_i, t)}{dt} = \mathbf{F}_i(\mathbf{r}_i, t), \quad \frac{d\mathbf{r}_i(t)}{dt} = \mathbf{v}_i(\mathbf{r}_i, t), \tag{1}$$

where $\mathbf{F}_i$ is total force acting on particle i with mass m_i at position $\mathbf{r}_i$ and with velocity $\mathbf{v}_i$. The outcome is a time-dependent record of particle positions, or in other words, a trajectory. Thermodynamic and kinetic properties – both equilibrium and time-dependent – can subsequently be calculated based on positions and momenta of the particles, as well as from the energy of the system. The latter is evaluated based on an empirical energy functional, that is, a force-field, which can be constructed to model interactions occurring at different scales, from atomistic detail level (bonds, angles and charge distribution at molecular level), all the way to interstellar motion of planets (gravitational forces). Here, the relevant particle-based modelling scales range from atomistic detail to mesoscale. The MD method is covered in detail in the books [67,68].

In the basic MD algorithm, the total energy is, to numerical accuracy, conserved. The modelling corresponds to microcanonical ensemble (NVE ensemble). However, temperature and pressure regulation, for description of, e.g., the isobaric-isothermic (NpT) ensemble conditions, often more relevant in biopolymer systems, can be implemented using thermostat and barostat algorithms. MD also allows including forces resulting from external fields, such as electric or magnetic field, and energy flows, such as heat sinks and sources of vibrations.

All-atom approaches in molecular dynamics

In atomistic detail modelling relevant to biopolymers, most commonly used force-fields consist of a sum of energy terms associated with covalent chemical bonds, bond angles, bond dihedrals, and non-bonded interactions, such as electrostatics [78]. For computational efficiency, the interactions are constructed as simple pairwise contributions assuming harmonic dependency (for angles three-body, and for dihedrals sometimes also higher terms are considered) [68,79]. Atomistic detail force-fields include a number of fitting parameters that model the effect of, e.g., atomic radii, charge distribution, equilibrium bond lengths, bond angles, and dihedral angles, on the total effective potential energy [80]. The corresponding interaction coefficients in the force-field are typically obtained based on fitting to quantum mechanical calculations or to experimental outcomes, such as lattice parameters, spectroscopic data, or larger scale thermodynamic properties [57,80]. The parameters vary in value across different force-fields [57,80]. The field of atomistic detail modelling of biopolymers, including appropriate force-fields and their accuracy assessment, is vast, and warrants its own review. For example, Refs. [57,80] survey force-field status at general level, while protein force-fields have been reviewed in Ref. [81]. Below, we consider recent directions.

As ever, parametrization and assessing the accuracy of molecular simulations remain a challenge [82,83]. Another limiting factor for biopolymer modelling is the short accessible time and length scales in atomistic detail modelling, Figure 1. In recent years, the most popular biomolecular force-field families have experienced updates improving their accuracy, but also making them more system specific. Increasing the atomistic detail molecular modelling significance for biopolymer modelling, the enhanced accuracy, together with modern advancements and large-scale parallelization in molecular modelling codes [84,85], have enabled μs and in some cases even ms range simulations of all-atom native protein structures and their function, including probing of transient states via enhanced sampling methods [86,87]. Traditionally, biomolecular force-fields have suffered in accuracy due to the lack of polarizability (representation of the molecular charge distribution by fixed point charges) [88]. MD force-fields have advanced also in this sense: more robust polarizable force-fields to capture, e.g., the stabilizing effects of polarization on protein secondary structure formation, have been developed [88–90].

A notable methodological advancement in recent years has been the emergence of constant-pH MD methods. While traditional atomistic detail MD considers molecular charge distribution, also at the level of protonation, fixed, approaches that allow accurate description of the changes in the amino acid protonation states caused by pH have been recently developed [91–94]. These

methods, which rely on knowing the pKa values of the ionizable groups, are highly relevant for biopolymers, and have been tested, e.g., for proteins, nucleic acids, and small peptides [95,96]. Notably, the neighboring groups influence the pKa values of the ionizable groups, which for biopolymers can cause significant pKa shifts [97]. While polarization effects and improving polarizable force-fields [98,99] remain a pressing challenge, constant pH approaches offer an interesting, recently opened, research ground for methodological advancements.

The choices made in functional form and parametrization of the atomistic detail MD force-fields influence the modelling outcomes. For example, protein conformations for denatured proteins by common all-atom MD force-fields, such as CHARMM and AMBER, are typically overly compact and vary between force-fields [87,100]. This results from the interaction parameters being derived mainly based on folded biomolecular structures and short peptides. Consequently, several recent improvements address intrinsically disordered proteins, see e.g. Refs. [101–103]. Retuning non-bonded interactions can better balance the forces associated with, e.g., salt bridge formation and hydrophobic interactions between non-polar residues, contributing to protein 3D-structure formation [104]. Another challenge for atomistic detail force-field accuracy are the nucleic acids DNA and RNA, see e.g. Refs. [105–107].

Since the predicted outcome may depend on the interactions model, a common research direction is force-field comparison, especially force-field prediction comparison with experiments. For example, predictions by multiple force-fields of pH-induced conformation changes in poly L-lysine and poly L-glutamic acid chains [108], B-DNA [105] or intrinsically disordered proteins [109,110], have been compared against experiments. Notably, ion interactions with biomolecules, including biopolymers, depend on the interactions model choice, and the usage of corrections is warranted for accuracy [111,112]. The comparisons show that force-field and parameter choices in atomistic detail modelling should consider the original reference systems used in the parametrization, and the type of verifications performed. Additionally, the modelling predictions should be tested against experimental data when possible.

Direct application of atomistic detail MD to biopolymers is extremely popular, with research targets being both on structure, dynamics, as well as at function level. Most works focus on biological systems with much less focus on materials applications, except in the cellulose directions [61,62,64]. For protein-based materials, a particularly relevant aspect is the hierarchical structure, and its effect on the materials assembly and characteristics. Some examples addressing this have focused on silk-like proteins. For example, a combination of experiments and all-atom MD simulations revealed that the nonlinear response of silk threads to stress is crucial to localize load-induced

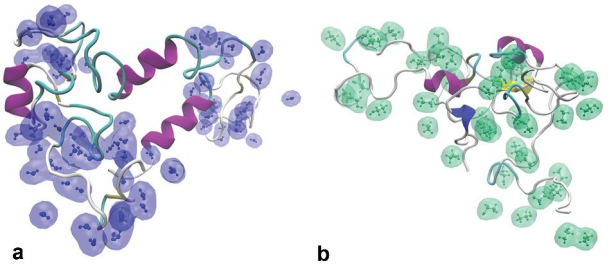

Figure 2. Example of using all-atom MD simulations to extract the effect of solvent environments on protein interactions. Distribution of a) water molecules (blue color) in 94% ethanol concentration aqueous solvent system and of b) ethanol molecules (green color) in 20% ethanol concentration aqueous solvent system. The visualized solvent molecules correspond to those located within 0.25 nm cutoff distance from the protein (considering all atoms of both the solvent molecule and the protein). Solvent clusters are highlighted in the visualization by transparent shading. Figure reprinted from Ref. [116] (CC BY-NC-ND 4.0).

deformation, resulting in mechanically robust spider webs [113], the stress dependency of silk-like protein assemblies [114], and that multiple attractive regions with different strength in the flexible silk-like protein lead to bicontinuous network structure, potentially bearing influence in fiber formation [115]. Furthermore, interesting for protein materials, a combination of all-atom MD and experiments elucidates in Ref. [116] the influence of ethanol as solvent additive on protein aggregation, but also the changes in microscopic solvation environment and in secondary structure, along with the molecular-level origins of these. The protein species of interest in the work is spidroins, the main proteins of silk. The work demonstrates an application of using atomistic detail MD to gain insight to alcohol treatment of proteins, which is a common processing step: Figure 2 demonstrates atomistic detail MD-derived local solvation and the distribution of the solvent around the protein at different ethanol concentrations of the aqueous solvent in the work [116]. Specifically, as ethanol distributes differently around the protein at different solvent additive concentrations, its effect of significantly weakening hydrophobic interactions by solvating hydrophobic regions provides a tuning handle to assembly, and materials properties [116].

Besides silk-like protein materials, also other protein materials, such as elastin-like peptides and their lower critical solution temperature response in materials formation has received attention, both at atomistic and CG detail [117–120]. Mechanical response of collagen fibers has been examined thoroughly in Refs. [121–123]. Also polypeptides [108,124–126] and bioinspired topics, such as energy dissipation in protein materials, have received computational attention [127].

Another direction receiving attention is biopolymer adsorption, which is often studied in atomistic detail due to the scale of interactions. For example, peptide adsorption on silica nanoparticle surfaces has been mapped as a

function of pH, particle diameter, and peptide electrostatic charge [126,128], but also in terms of silica surface structure [129]. Although topics such as molecular level dependencies of film formation and collective effects in adsorption response would be interesting, the modelling length and time scales of atomistic detail modelling remain prohibitively limiting.

The rather limited modelling length and time scales of atomistic detail modelling, Figure 1, can be expanded by combining the approach with larger scale modelling or experiments. Although appealing, the former combination remains relatively rare for biopolymer systems, the main challenge being interfacing the models that have different description scales. Successful examples include, e.g., the combination of two theoretical approaches in Ref. [130], where the effects of polymer conjugation on hybridization thermodynamics of oligonucleic acids was addressed by both CG Langevin and atomistic detail MD simulations [130]. Likewise, Ref. [131] showed that specific material recognition by small peptides is governed by local solvent density variations at the solid/liquid interfaces. The latter work mainly focuses on the origin of the selectivity of the binding motif RKLPDA for Ti over Si combining metadynamics and steered MD simulation as modelling approaches in atomistic detail. An interesting multiscale modelling combination of atomistic to continuum level modelling of mussel adhesion proteins is presented in Ref. [132]. An additional example is the combination of experiments, all-atom MD simulations, and mesoscopic dynamical modelling used to address the phase response of chitosan/poly(ethylene oxide) blends [133].

Coarse-grained approaches in molecular dynamics

CG force-fields consider the interactions at a level that view regions in the molecular system by effective smoothened description, averaging the effect of both spatially and temporally most localized interactions [134–137]. This typically enables using simpler and thus computationally cheaper analytical interaction potentials compared to fully atomistic detail interaction models [134,138]. Also the use of cut-off-based interactions and soft potentials provide computational advantage, naturally at the cost of loosing information that would rise from the details that were smoothened in constructing the effective CG model [136,138]. The practical consequence is that simulations of significantly larger systems and longer time periods than in full atomistic detail are feasible [134,136]. For molecular level coarse-graining, typical system dimensions are up to 100 nm, and can include millions of particles [139,140]. The observable time scales extend with relative ease to μs range and above.

Key in CG model construction is the coarse-graining of the atomistic or molecular level details of the biopolymers to make the CG beads or interaction units, and the definition of the interaction features [134,136,140]. The interaction units, in practise, the degree of coarse-graining, is commonly

a compromise between description detail and achievable system size and time scales [141]. The effective interactions, i.e. development of accurate and transferable CG MD force-fields, can be divided into two main approaches: bottom-up structure-based coarse-graining, in which the effective CG potentials are based on reference atomistic detail MD simulations, and top-down thermodynamics-based coarse-graining, in which the effective interactions are fitted to reproduce key experimental observables (such as thermodynamic properties) of the modelled system [138,141–143]. The former approach retains better the chemical characteristics of the target system, but the latter often produces more transferable potentials [138,141,142]. Quite common in CG model construction is the combination of the two approaches to iteratively tune the CG potential parameters. Examples include a unified CG model of biological macromolecules based on mean-field multipole – multipole interactions able to describe structure and energetics of proteins, nucleic acids, and polysaccharides [144], but also a hybrid model aimed at bridging the gap between atomistic and CG modelling of surfactants in apolar solvents [145].

While CG approaches give access to significantly larger structural features and longer time scales of the dynamics of biopolymer systems, a major drawback of all CG MD models is that the entropic contributions in the simulated systems decreases significantly as a function of the coarse-graining level, since mapping groups of atoms into interacting beads reduces the degrees of freedom [137,138]. This is often counterbalanced by increasing enthalpic contributions [146]. The phenomenon is even more evident for CG force-fields that employ implicit solvent models, such as Dry Martini [139]. In it, the solvent entropy loss is compensated by significant tuning of the Lennard-Jones interactions between the CG beads to better capture, e.g., hydrophobic effects and charge screening. By construction, the CG models are thus much more specific to parametrization conditions, such as temperature and the specific system, a fact that should be considered in their use [137,138,142].

For biopolymers, perhaps the most used CG MD force-field is the Martini model [147,148]. Similarly to other broad scope, transferable CG force-fields, it assumes that groups of atoms can be represented by specific CG bead types. One CG Martini bead represents on average four heavy (i.e. non-hydrogen) atoms, however a higher resolution mapping is used for cyclic molecules. Interactions between beads are parametrized using a combination of top-down and bottom-up approaches. Non-bonded interactions are modelled by a Lennard-Jones potential parametrized against experimental thermodynamic data, such as free energies of partition. The bonded interactions between the beads are tuned to match atomistic MD distributions. Solvent effects are modelled using explicit solvent beads, which provides transferability of the model between water and membrane phases, at the cost of reduced computational efficiency. While originally parametrized for lipids [147–149], Martini has been

expanded to encompass other biomolecules, including proteins, DNA [150], RNA [151], polysaccharides and carbohydrates [152–158], as well as, other biobased and synthetic polymers [159–162]. Recent reparametrization of the Martini force-field rebalances the interactions and introduces new bead types to better capture hydrogen bonding and electronic polarizability [146]. Additionally, Dry Martini [139] implemented an implicit solvent approach to gain a significant speed-up (by a factor 1–2 for large 100 nm lipid vesicles). However, the formalization of the model, specifically the lack of purely repulsive interactions, makes it incapable of modelling soluble proteins or equilibrium between, e.g., membrane-bound and dissolved populations of compounds.

Besides Martini, there exists also a number of other widely used CG approaches in biopolymer modelling. For example, the SIRAH CG force-field [163–165] avoids the constraints needed in Martini for secondary structure of proteins. Besides proteins and DNA, it provides access to CG modelling of protein-DNA complexes [166]. Predictions of UNRES model [144] have been demonstrated for a wide set of biomolecules. Due to its multiscale structure, also cellulose has been the target of several successful CG models [62]. SURPASS [167] is a low-resolution CG model for peptide and protein modelling. PRIMO model, for both proteins and nucleic acids, has been extended also to cover membrane protein modelling [168,169]. Also a growing interest in designing CG force-fields via machine learning methods exists. The approach has been demonstrated for generating atomistic interaction potentials based on quantum mechanical calculations, and similar frameworks have been developed also for CG-force-fields [170–172]. References [138,142,173,174] are recent reviews in this field.

The major challenge with CG force-field approaches is the accurate representation of the effective pair potential between CG beads [134]. If parametrized bead-wise, the interaction depends on the chemical environment, that is, whether the bead is immersed in aqueous solvent or buried in an apolar environment, e.g., in a protein core [134,136]. One solution is using many-body potentials to better describe interactions in different chemical surroundings and also within densely packed structures, such as protein interiors [172,175,176]. Additionally, the inherent loss in chemical and fine-grained detail in CG approaches often hinders investigation of highly localized phenomena, such as molecular recognition and reorganization of binding sites, but also charge-charge interactions, including localized effects of ions [138,146]. Recently, hybrid models where regions of interest – often the biologically most relevant regions of molecules – are represented in atomistic detail, and the rest of the system is modelled at CG level [177–180]. Such hybrid all-atom/CG approaches combine the advantages of both, with local accuracy and chemical specificity yet at reduced total computational cost due to cheaper CG regions.

Examples of applications of CG modelling to biopolymers include, e.g., the effect of the variation of oligonucleic acid backbone chemistry on the hybridization/melting thermodynamics of oligonucleic acids [181], but also the effect of oligonucleic acids design on the thermodynamics and assembly of multi-arm oligonucleic acids – star polymer conjugates [182]. Also collagen mechanical properties have been mapped [183]. On the other hand, the interaction with interfaces is also accessible by CG MD, such as in Ref. [184], where substrate patterning and film morphology, with focus on lamellar phase behaviour of copolymers under different heating cycles and substrate conditions, has been addressed by means of simple CG bead-spring model. Reference [185] presents an interesting approach to intrinsically disordered proteins at interfaces, integrating all-atom modelling to generate CG model for the proteins. Other examples of CG modelling combined with atomistic detail MD simulations are the lower critical solution temperature examinations of elastin-like peptides [118,120]. Collagen-mimetics and their fibril formation were modelled in Ref. [186]. Related, tropoelastin self-assembly into fibrils is examined by CG Martini approach in Ref. [187]. Also the assembly of poly(ethylene glycol) polymers and PEG-conjugated lipids in bulk [188,189] and their interfaces with proteins or surfaces [190,191] has received significant attention in CG modelling detail due to the bioengineering and drug delivery applications. Moreover, a new minimal CG MD model that takes into account intrinsically disordered proteins heterogeneity in nuclear pore complexes has been developed in Ref. [192], and benchmarked on experimental data of single-molecule interactions between intrinsically disordered proteins and nuclear transport receptors. Furthermore, Ref. [193] presents a review of colloid and protein adsorption CG models.

In conclusion of this section, we suggest consulting the recent review, Ref. [194], in which models employing diverse coarse-graining resolutions enhance understanding of the mechanisms that govern chromatin organization. Figure 3 provides a visual summary that shows the various modelling scales commonly used in studying the regulatory mechanisms influencing chromatin structure [194]. Notably, the Authors anticipate an increase in the use of data-driven methods, coupled with experimental data, and expect this to reveal groundbreaking insights on how the functional organization of chromatin is both sustained and regulated across all scales.

4. Dissipative particle dynamics in modelling of biopolymers

Extending the achievable modelling length and time scales significantly from the deterministic atomistic and CG MD simulations, Figure 1, DPD is a soft-core potential, CG, particle-based simulations model, which examines the time evolution of a system of particles reproducing fluid dynamics modes

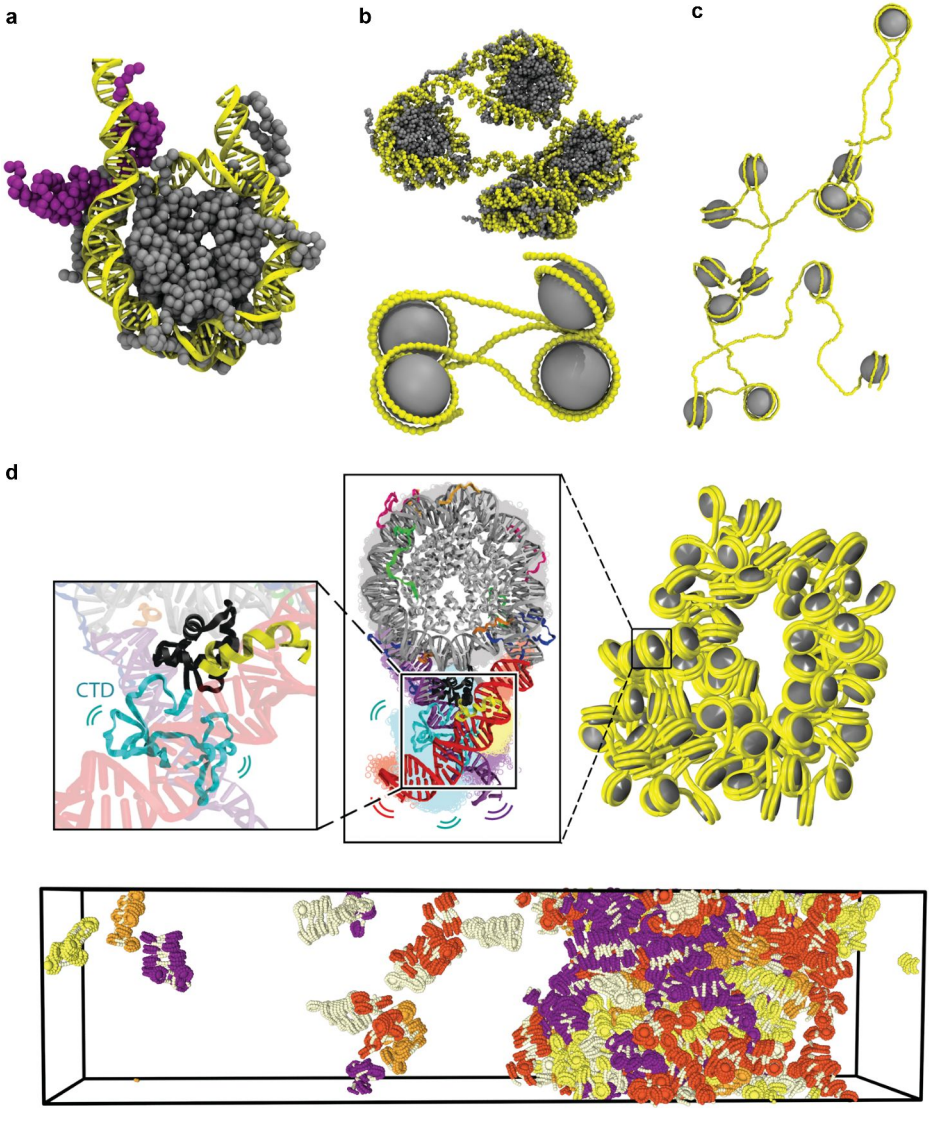

Figure 3. Different scales of modelling allowing the investigation of local and global mechanisms of chromatin structure regulation. Panel a) presents near-atomistic approaches for studying the detailed modulation of nucleosome structure and dynamics by interacting partners, such as transcription factors. The approach follows such as Ref. [195]. In panel b), near-atomistic and sub-nucleosome models are used to reveal physical and molecular characteristics that make the structure of chromatin transform, following such as presented in Refs. [196,197]. In panel c), the effects of DNA mechanical properties changes stemming from sequence or epigenetic marks are modelled by a hybrid model, following the presentation of Ref. [198]. Panel d) summarizes multi-scale approaches bridging atomistic features of nucleosomes to the mesoscale organisation of chromatin and its phase separation. The presentation follows similar to Refs. [199,200]. Figure reprinted from Ref. [194] (CC BY-NC-ND 4.0).

and liquid response [201,202]. Its operation range is in the mesoscale structural and dynamics region, capturing assembly structure and morpohology

changes, as well as large scale structural flows [202]. Like the atomistic and CG MD approaches, also DPD is based on integration of Newton's equations of motion, Eq. 1. In DPD, analogous to other CG approaches, each particle (usually referred to as bead) in the system represents a cluster of atoms or more accurately a region of the modelled system. This results in significant reduction of degrees of freedom, which together with the soft-core format of the interactions potential, allows the simulation of length and time scales that are orders of magnitude larger than those achievable by previously discussed methods.

In DPD, the total force $\mathbf{F}_i$, acting on bead i [201,202], is formulated as

$$\mathbf{F}_i = \sum_{j \neq i} (\mathbf{F}_{ij}^{\mathrm{C}} + \mathbf{F}_{ij}^{\mathrm{D}} + \mathbf{F}_{ij}^{\mathrm{R}}), \tag{2}$$

where $\mathbf{F}_{ij}^{\mathrm{C}}$ denotes the conservative, $\mathbf{F}_{ij}^{\mathrm{D}}$ the dissipative, and $\mathbf{F}_{ij}^{\mathrm{R}}$ the random force, respectively, and where the index j represents all other beads in the system. This approach assumes pairwise interactions, which are truncated at a cutoff distance r_{c}. Both of these aspects contribute to the computational efficiency of DPD in comparison to many other methods. Even more importantly for computational efficiency and the extended time scales reachable by DPD, $\mathbf{F}_{ij}^{\mathrm{C}}$ corresponds to a simple repulsive soft-core potential, which allows the use of a significantly longer integration time step (in comparison to, e.g., force-field based MD simulations). The soft potential also leads to enhanced relaxation dynamics. Altogether, these result into overall increased temporal and spatial reach.

The use of a soft-core potential as the conservative force component can be justified by considering that the interactions between groups of several hard-core particles (Lennard-Jones type interactions) result in a soft effective interactions potential [203]. The conservative force is defined as

$$\mathbf{F}_{ij}^{\mathrm{C}}(r_{ij}) = \begin{cases} a_{ij}(1 - r_{ij})\hat{\mathbf{r}}_{ij}, & r_{ij} < r_{\mathrm{c}}, \\ \mathbf{0}, & r_{ij} \geq r_{\mathrm{c}}, \end{cases} \tag{3}$$

where a_{ij} is the conservative repulsion parameter between particles i and j, controlling the miscibilities of the different components of the system, $r_{ij} = ||\mathbf{r}_i - \mathbf{r}_j||$ their distance (commonly expressed in units of the cut-off distance r_{c}), and $\hat{\mathbf{r}}_{ij} = \mathbf{r}_{ij}/r_{ij}$ the unit vector giving the force direction. Notably, r_{c}, which sets the range of interactions, is determined based on the coarse-graining scale of the system, i.e. the number of atoms or solvent molecules represented by each bead. In standard DPD, all interacting beads, regardless of bead type or modelled chemical species, are considered to be of the same size (both volume and mass).

$\mathbf{F}_{ij}^{\mathrm{D}}$ and $\mathbf{F}_{ij}^{\mathrm{R}}$ are together responsible for the conservation of total momentum in the system, and incorporate the effect of Brownian motion into the larger length scale. These two forces read

$$\mathbf{F}_{ij}^{\mathrm{D}}(r_{ij}, \mathbf{v}_{ij}) = -\gamma\omega^{\mathrm{D}}(r_{ij})(\hat{\mathbf{r}}_{ij} \cdot \mathbf{v}_{ij})\hat{\mathbf{r}}_{ij} \tag{4}$$

and

$$\mathbf{F}_{ij}^{\mathrm{R}}(r_{ij}) = \sigma\omega^{\mathrm{R}}(r_{ij})\xi_{ij}\Delta t^{-1/2}\hat{\mathbf{r}}_{ij}, \tag{5}$$

where $\mathbf{v}_{ij}$ is the relative velocity between the two considered beads, and γ and σ are the friction coefficient and noise amplitude (defined below), respectively. $\mathbf{F}_{ij}^{\mathrm{D}}$ and $\mathbf{F}_{ij}^{\mathrm{R}}$ also encompass the distance-dependent weight functions for the dissipative force $\omega^{\mathrm{D}}(r_{ij})$ and the random force $\omega^{\mathrm{R}}(r_{ij})$, as well as the random number ξ_{ij} with zero average and unit variance (Gaussian white noise).

Coupling $\mathbf{F}_{ij}^{\mathrm{D}}$ and $\mathbf{F}_{ij}^{\mathrm{R}}$ provides a thermostat to the simulation: an increase in the noise causes particle velocities to increase (heating up of the system), which is countered by the dissipative contribution slowing down the particles correspondingly. Additionally, if $\xi_{ij} = \xi_{ji}$, Eqs. 4 and 5 form a pair-wise Brownian dashpot, ensuring conservation of momentum. Furthermore, the following relationships exist

$$\omega^{\mathrm{R}}(r_{ij}) = \sqrt{\omega^{\mathrm{D}}(r_{ij})}, \quad \sigma = \sqrt{2\gamma k_{\mathrm{B}}T}, \tag{6}$$

where T is the absolute temperature and k_{B} the Boltzmann constant. As a result, one of the weight functions of Eq. 6 can be chosen arbitrarily, and the amplitude of the random force is related to the friction coefficient γ. Generally, $\omega^{\mathrm{R}}(r_{ij}) = 1 - r_{ij}/r_{\mathrm{c}}$, for $r_{ij} < r_{\mathrm{c}}$, is used, based on the original publication by Groot and Warren [204].

For simulating biopolymers, the basic DPD approach of Eq. 2 is typically augmented by an additional force term $\mathbf{F}_i^{\mathrm{S}}$, corresponding to a spring force between two consecutive beads in the same polymer chain, reading

$$\mathbf{F}_i^{\mathrm{S}}(r_{ij}) = -\kappa \sum_{j^*} (r_{ij} - r_0)\hat{\mathbf{r}}_{ij}, \tag{7}$$

where κ is the spring constant, r_0 the spring equilibrium distance, and j^* indicates the nearest neighbours in the chain. Besides the spring force corresponding to a harmonic potential, a common way to define the bond is using a finite extensible nonlinear elastic (FENE) potential [205].

In comparison to the previously covered simulation approaches, DPD is a powerful technique in reaching extended length and time scales in modelling

biopolymer solutions [202]. However, due to the simplifications involved in model construction and algorithm setup, the approach is also lacking in ability to describe many directions in biopolymers and their assemblies. For example, in conventional DPD simulations, perpendicular velocity vector and distance vector lead to zero dissipative force [202]. This effectively excludes the possibility of shear forces between pairs of particles. This has been remedied in smooth DPD approaches [206]. Furthermore, the repulsive form of the conservative force, Eq. 3, implies that, e.g., liquid-vapor interfaces cannot be modelled by conventional DPD [204]. Beyond the standard DPD, many-body DPD can be used to model such cases [207]. In many-body DPD, the response is captured by density-dependent many-body conservative potential with attractive and repulsive terms. Interesting for biopolymer modelling, DPD approaches extend also to capturing protein structure [208,209].

In biopolymer modelling, DPD reaches time scales associated, e.g., with bulk self-assembly and morphological transitions that are typically outside the reach of even CG MD. Especially interesting for materials applications is the stimuli responsive wide range of self-assembly morphologies, such as spheres, vesicles, rods or even hierarchical morphologies, that copolymer-like assemblies readily exhibit [210]. Assembly morphologies of di-block copolymers in both bulk melts and solutions are well-known to depend strongly on the block segment length ratio and component miscibilities [211].

In the latter, a systematic study of the self-assembly behavior of poly(1,2-butadiene)-b-poly(ethylene oxide) (PB-b-PEO) block copolymer in [Bmim][PF6] ionic liquid (IL), reported here in Figure 4, is provided. Both PB and PEO can be biobased, and are thus used here as DPD example to represent the ability of the model to resolve assembly phase diagrams: a vast variety of assembly structures, such as spherical micelles, rodlike micelles, entangled cylinders, sheets, branched lamellae, lamellae, platelets, tubes, and IL microphase structures, as a function of polymer concentrations and polymer block ratios were reported [211]. DPD modelling have allowed mapping these and other dependencies, relevant for biopolymers as well.

Furthermore, Seki et al. [212] examined the self-assembly of peptide amphiphiles via DPD approach, reporting the temperature dependency response of the micelle shape transitions from spherical to worm-like by depicting the temperature shift associated hydration change as simple tuning of surfactant – solvent interaction parameters. Similarly, the role of molecule shape, i.e. branching and cyclic structures, on formed self-assembly structures and assembly phases has been investigated for bio- [213,214] and synthetic [215–220] block copolymers.

A significant recent focus area in the modelling of equilibrium assembly of biopolymer systems has been drug delivery, most commonly small molecule release from self-assembled vesicle-like structures [219–222]. The

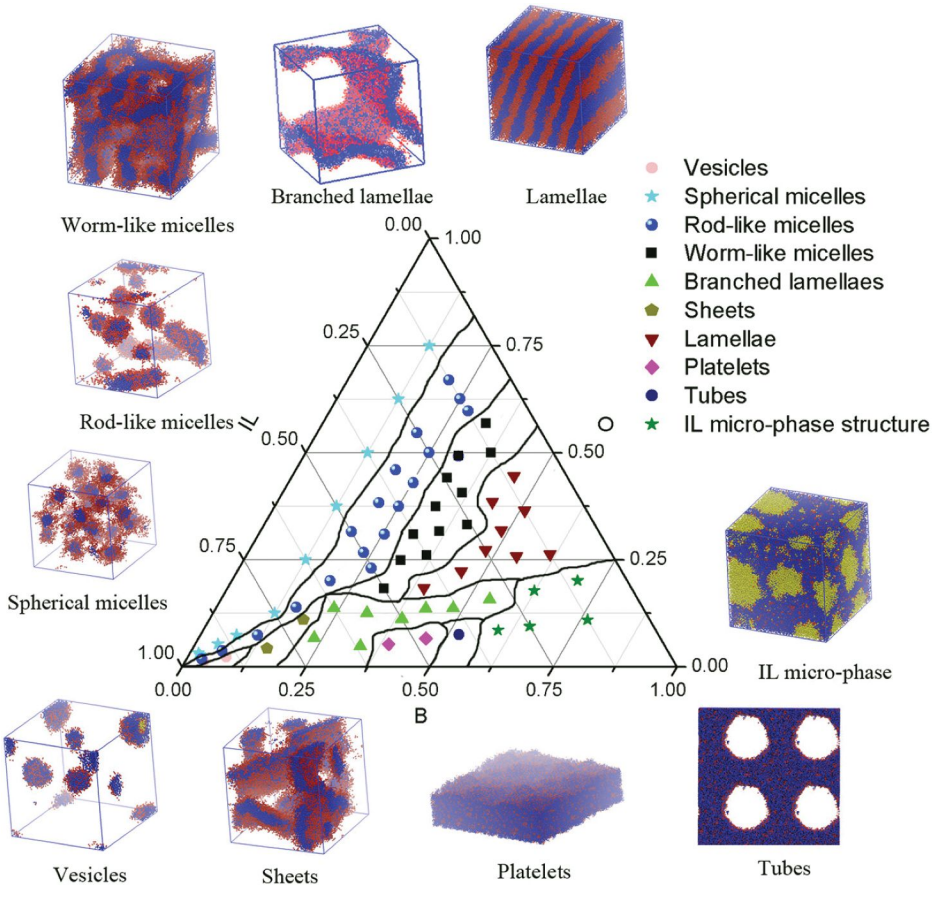

Figure 4. Ternary phase diagram in vol % and corresponding structures at 298 K by DPD simulations. Blue, poly(1,2-butadiene) (B) beads; red, poly(ethylene oxide) (O) beads; and yellow, [Bmim][PF6] ionic liquid (IL) beads. The concentration unit of the phase diagram is volume fraction (vol %). Reprinted with permission from Ref. [211]. Copyright © 2016, American Chemical Society.

mesoscale approach allows capturing structural features and dynamics. Examples include the bottom-up DPD model based on atomistic simulations for self-assembling PAE-g-PEGLA vesicles with doxorubicin hydrochloride loaded into the vesicle core [221]. These results demonstrated the carrier to be easily tunable via solvent phase, solvent exchange rate, polymer concentration, and polymer block lengths. Release of the drug in response to a pH change and protonation PAE block was achieved by tuning the DPD interaction parameters. Also block-co-polyelectrolyte-based self-assembly carriers have been modelled [219,220], with variables covering block length ratio, polymer concentration, polymer chain length, and polymer block – solvent selectivity.

The hierarchical structure of many biopolymer assemblies is well-suited for DPD, as long as the assembly rises from characteristics captured by the

effective bead-bead interactions and not from, e.g., highly localized interactions, see e.g. Ref. [214]. Namely, the CG description of each individual molecule can be retained, but the larger length scale structures forming during longer (μs) time scales can also be captured thanks to the soft interactions. Examples of higher scale self-assembly of copolymer micelles into more complex hierarchical structures include, e.g., the study by Zhuang et al. [223], in which the solvent change drives self-assembly of poly(γ-benzyl-l-glutamate)-graft-poly(ethylene glycol) (PBLG-*g*-PEG) micelles into nanowire structures. Related, giant fibers have also been demonstrated by DPD approaches. In particular, hydrophobic dimerization promoted oligomeric strand formation in Ref. [224]. DPD approaches have also been used to examine silk protein fiber assembly, processing conditions and design parameters, in particular by considering the proteins as multi-block copolymers [214]. With appropriate degree of coarse-graining, also protein structure can be captured [208,209].

The high level of coarse-graining achievable by DPD, and its extended time scales, have been used to examine large scale self-assembly phenomena in biopolymer systems. Examples include protein complexation and aggregation, both in solution and in two dimensional environments. For example, Li et al. [225] modelled the aggregation of protein complexes in a lipid bilayer, demonstrating entropy-induced attraction between protein complexes with complementary shape. Here, naturally the entropy considerations are subject to the coarse-graining in the model. Chen et al. [226] tuned the co-operative self-assembly of polymer solutions into rods, curved rods, and toroids, with the mixing ratio of linear polymers, branched polymers, and water content, as study variables. DPD has also been used to study self-assembly of proteins and amphiphilic molecules in confinement with elastic boundaries, such as micelles or lamellar vesicles [227]. The findings reveal, e.g., that confined geometry, such as vesicle curvature, may give rise to interesting self-assembly structures not observed in bulk phase, such as U-like and toroidal vesicles [227]. An interesting approach to modelling protein secondary structure effects is presented in Ref. [228], where, based on atomistic detail MD simulations, a DPD approach to capture polyalanine folding into a stable helical conformation is considered. The approach reproduces the folding of polypeptides for different lengths, including bundle formation for sufficiently long polypeptides.

DPD also allows examining patterning on surfaces. The time scales and size reach in DPD is sufficient to map block copolymer self-assembly to, e.g., nanopatterns, such as stripes on surfaces, charting the effect of miscibility differences between the components [229]. Interestingly, DPD also expands to effective description of, e.g., the effect of reaction rate kinetics in polymerization reactions on surface brush growth by considering surface modifications [230].

While the energy barriers in DPD are typically significantly lower in comparison to classical MD due to the CG and soft character of the potentials, it is worth noting that the method still suffers from kinetic trapping into local minima. This is most prevalent at low temperatures, where most stable structures may only be obtained via enhanced sampling techniques, such as replica exchange, as demonstrated by Kobayashi et al. [231] for threadlike surfactant micelles.

DPD also offers interesting prospects in mapping dynamics and temporal reorganization of biopolymer systems, including flows. Due to the conservation of fluid dynamics, DPD has been widely used to examine biopolymer response to external flow fields and to particular geometries. For example, Posel et al. [232] simulated the flow and aggregation of rod-like proteins as solution in polymer coated pores and slits. The modelling revealed that tuning solvent quality controlled a phase transition of the polymer coating, with a stretched polymer brush hampering protein solution flow promoting protein aggregation. Lin et al. [214] simulated the self-assembly of hydrophobic/hydrophilic block copolymers based on silk proteins under shear flow to mimic spinning processing. The findings revealed that larger micelles, induced by increase in hydrophobic domain size, elongate under shear flow to form percolating fibre networks, which resulted in increased stability.

In addition to explicitly including forces arising from external fields, such as shear [206], classical DPD has been expanded to cover also additional features, such as electrostatics [233,234] and polarizability [235–237]. For charges, a smeared charge approximation is proposed and used for the exploration of micellization response of anionic and cationic surfactants, and their mixtures, in solution [238]. For polarizable DPD approaches, Peter et al. [235] introduced charged Drude DPD particles in the spirit of their prior polarizable DPD water [239]. While including polarizability reduces the achievable level of coarse-graining and computational efficiency, the model was able to accurately replicate protein structural parameters, as well as capture experimentally observed folding pathways and native protein structure [235].

5. Langevin and Brownian dynamics in modelling of biopolymers

Stepping further into effective interactions and coarse-graining of biopolymers, Langevin, originally derived in Ref. [240] and thoroughly described in Ref. [241], and Brownian dynamics (BD) [242], are bead-based approaches that model the effective dynamics of a system resulting from the presence of a solvent. Both methods are fundamental numerical techniques for simulating both equilibrium and non-equilibrium phenomena of micro- and meso-scopic systems. BD simulations applied to biological molecules, including biopolymers, have been recently reviewed in Refs. [243,244]. Generally, Langevin dynamics mimics the effects rising from a viscous solvent, while

BD is its overdamped limiting case, in which the particles do not undergo acceleration, or in other words, have no inertia [241].

Notably, while Langevin dynamics captures the effect of solvent, this is limited to effects rising from stochastic collisions, excluding, e.g., dielectric screening, proper hydrodynamic effects, or solvation effects, such as hydrophobicity [241]. Consequently, systems representing biopolymers typically encompass chains of beads, and in addition to the plain Langevin dynamics, described below, extra interaction terms, corresponding to effective interplay between particles, need to be introduced. These capture, e.g., hydrophobicity at an effective level or interactions between charges, but also the constraints holding the chain of beads together.

Langevin dynamics

To formulate the Langevin dynamics approach [241], let us consider a particle with mass m and radius R_1 suspended in a fluid where the solvent molecules have a radius R_2. If $R_1 \gg R_2$, one can assume that the suspended particle experiences a very large amount of collisions by the solvent molecules. This assumption is readily valid for typical molecular to colloidal particle scales, for which $R_1 \approx$ nm-μm, and for small solvent molecules, such as water or gases, for which $R_2 \approx 10^{-1}$nm. The effect of collisions on the particle at time t can be captured by a random force $\boldsymbol{\xi}(t)$. The second major contribution to the dynamics of the particle is the friction it experiences moving in the solvent. For low Reynolds numbers (laminar flow), the friction force can be assumed to be linearly proportional to the velocity of the particle $\mathbf{v}(t)$. The governing equation of motion can be thus written as

$$m\frac{d\mathbf{v}(t)}{dt} = -\gamma\mathbf{v}(t)+\boldsymbol{\xi}(t), \tag{8}$$

where γ is the friction coefficient. For a viscous fluid, the friction coefficient $\gamma = 6\pi\eta R_1$, in which η is the viscosity of the fluid. The average of the noise term is $\langle\boldsymbol{\xi}\rangle = \mathbf{0}$, while its time correlation is $\langle\boldsymbol{\xi}(t)\boldsymbol{\xi}(t')\rangle = 6k_{\mathrm{B}}T\gamma^{-1}\delta(t-t')$, which corresponds to random white noise, where δ is the so called Dirac δ function. Rearrangement of Eq. 8 gives

$$\frac{d\mathbf{v}(t)}{dt} = -\frac{\gamma}{m}\mathbf{v}(t)+\frac{1}{m}\boldsymbol{\xi}(t), \tag{9}$$

which corresponds to the Langevin equation of motion [240]. It is important to reiterate that this equation neglects electrostatic screening and hydrodynamics. Furthermore, it describes the dynamics of a single particle immersed in a solvent. However, most practical systems are composed of $\mathcal{N}>1$ suspended particles. Consequently, additional contributions to the

forces experienced by each particle *i* in the system need to be considered. Most important are the interparticle interactions (in the case of biopolymer, including also eventual tether forces), but the additional contributions can also capture the effects of the solvent omitted in the basic Langevin formulation. The approach leads to $\mathcal{N}$ coupled equations of the form

$$\frac{d\mathbf{v}_i(\mathbf{r}_i,t)}{dt} = -\frac{\gamma_i}{m_i}\mathbf{v}_i(\mathbf{r}_i,t)+\frac{1}{m_i}\boldsymbol{\xi}_i(t)-\frac{\nabla\Phi_i(\mathbf{r}_i)}{m_i}. \tag{10}$$

Here, the force terms $-\nabla\Phi_i$ correspond to interparticle interaction potentials and external force contributions on the particles. The total potential Φ_i is generally defined as the sum of all force contributions in the system, namely

$$\Phi_i(\mathbf{r}_i)= V_i^{\text{ext}}(\mathbf{r}_i)+\sum_j \phi_{ij}(\mathbf{r}_i,\mathbf{r}_j)+\sum_{j,k} v_{ijk}^{(3)}(\mathbf{r}_i,\mathbf{r}_j,\mathbf{r}_k)+\sum_{j,k,l} v_{ijkl}^{(4)}(\mathbf{r}_i,\mathbf{r}_j,\mathbf{r}_k,\mathbf{r}_l)+\cdots. \tag{11}$$

In this, V_i^{ext} represent one-body external potentials (e.g. gravitation or the potential exerted by a container walls), and ϕ_{ij} describes the pair-wise interactions of the particles. In principle, triplet contributions $v_{ijk}^{(3)}$, and even higher order multiparticle interactions, such as $v_{ijkl}^{(4)}$, can be considered, but in most common approaches the standard procedure is to account only up to pair contributions.

For identical particles some indices can be dropped. Assuming the absence of external potentials, i.e. $V_i^{\text{ext}}(\mathbf{r}_i)\equiv 0$, and omitting the multiparticle interactions contributions, Eq. 10 obtains the most well known form for Langevin dynamics-based particle system simulations

$$\frac{d\mathbf{v}_i(\mathbf{r}_i,t)}{dt} = -\frac{\gamma}{m}\mathbf{v}_i(\mathbf{r}_i,t)+\frac{1}{m}\boldsymbol{\xi}(t)-\frac{\sum_j \nabla\phi_{ij}(\mathbf{r}_i)}{m}. \tag{12}$$

Altogether, Langevin dynamics provides an interesting CG approach of large-scale particle based simulations of biopolymers. As with all CG approaches, the challenge remains in interactions model construction (effective interactions) and matching the parameters to actual biopolymer systems. However, the approach is powerful in scaling-up both time and length scales, and allows mapping both assembly and dynamics. An example using CG Langevin dynamics simulations in a biopolymer setup can be found in Ref. [130], where the effects of polymer conjugation on hybridization thermodynamics of oligonucleic acids were addressed. Another interesting approach is provided by the combination of scaling arguments and low friction Langevin dynamics simulations to study the effects of macromolecular crowding on the collapse of biopolymers, and to characterize the polymer size

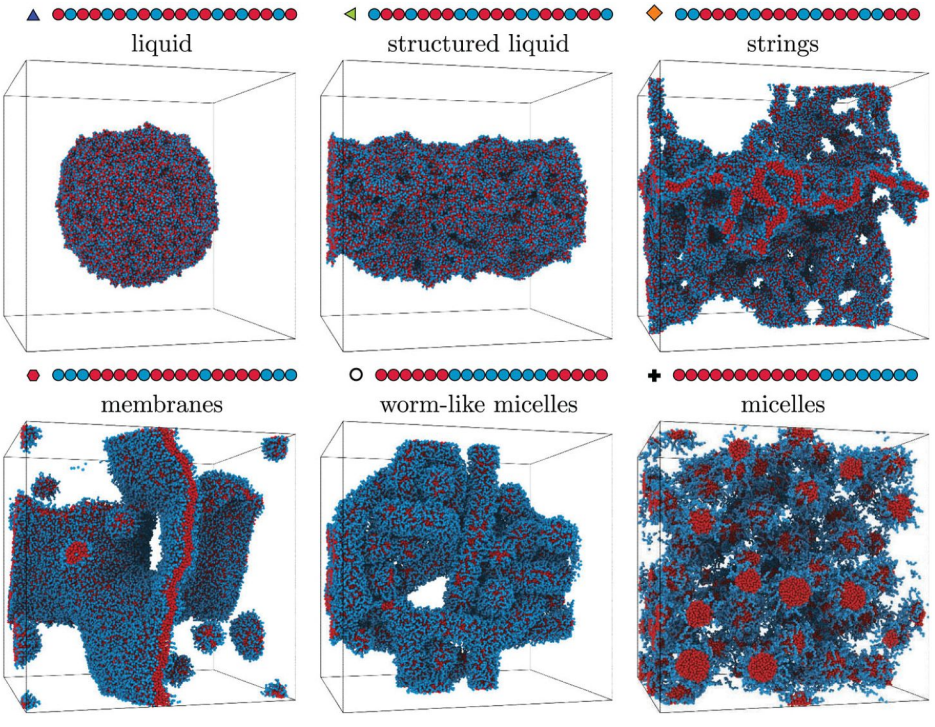

Figure 5. Assembly configurations rising in CG modelling of intrinsically disordered proteins with varying sequences at fixed concentration, temperature, and degree of hydrophobicity (red beads). The figure is presented to demonstrate the reach of Langevin and BD type CG modelling in the context of biopolymers, here proteins. Reproduced from Ref. [248], with the permission of AIP Publishing.

as a function of the volume fraction [245]. Furthermore, Langevin dynamics have been recently used to investigate protein diffusion in lipid bilayers [246].

Langevin dynamics approaches have also raised interest in the context of intrinsically disordered proteins, see e.g. Refs. [247,248]. In Ref. [247], a CG model including repulsive steric, attractive hydrophobic, and electrostatic interactions between residues was implemented. Reference [248] investigates liquid-liquid phase separation dependency on sequence via a coarse-grained model, reporting a rich phase behavior. Figure 5 demonstrates how this type of approaches can reveal assembly changes at the level of large scale structures ranging from liquid, structured liquid, strings, membranes, worm-like micelles, to micelles. Here, the changes are driven by minor alterations in the ordering of residues leading to variation of the hydrophobic/hydrophilic sequence.

Relevant to biological processes, sensor applications and molecular level switches, the structure and dynamics of an active polymer adsorbed on the surface of a cylinder has been addressed in Ref. [249]. Langevin dynamics

have also been coupled with hydrodynamic interactions between the polymer and the fluid [250] with findings addressing the electrophoretic transport of biopolymers through synthetic nanopores in quantitative agreements with experiments. Langevin dynamics also allows examining, e.g., cross-linked biopolymer networks with active motors [251]. The work demonstrates a pronounced network strain stiffening taking place with increasing shear deformation, mostly relevant for cytoskeletal networks. More generally, cytoskeletal networks, especially actin-based ones, are addressed by the extensive overview of theoretical and computational approaches for understanding the dynamic behaviors and underlying mechanisms of them in Ref. [252]. Langevin dynamics also allows modelling single protein conformations at constant pH [253].

Brownian dynamics (Overdamped equations of motion)

In the overdamped regime, i.e. particles without inertia, Eq. 12 reduces to

$$\gamma \mathbf{v}_i(t) = -\nabla \Phi_i(\mathbf{r}_i) + \boldsymbol{\xi}(t). \tag{13}$$

The assumption of no inertia is valid if the velocity correlations decay on a time scale $\tau = m/\gamma$ much smaller than the considered time scale t, i.e $t \gg \tau$. Equation 13 is a first order differential equation for which the time evolution can be solved numerically using, e.g., the Euler method. This approach for particle-based simulations is called *Brownian Dynamics* [242]. Since

$$\mathbf{v}(t) = \frac{d\mathbf{r}(t)}{dt} = \lim_{dt \to 0} \frac{\mathbf{r}(t + dt) - \mathbf{r}(t)}{dt}, \tag{14}$$

the time trajectories of the particles are obtained by recursive solving of

$$\mathbf{r}_i(t + dt) = \mathbf{r}_i(t) - \gamma^{-1} \sum_j \nabla \phi_{ij}(\mathbf{r}_i) dt + \delta \mathbf{r}_i, \tag{15}$$

where dt is the discrete integration time step, and $\delta \mathbf{r}_i$ are the random contributions to position sampled from a Gaussian distribution with standard deviation $\sqrt{6 k_B T \gamma^{-1} dt}$.

Also BD approaches have been used successfully to model biopolymer systems, see e.g. Ref. [254]. BD modelling has received significant attention in the context of examining crowded dynamics, e.g., in cells [255–257]. In biopolymer context, a large fraction of BD-based works focus on proteins, recently especially on liquid-liquid phase separation. For example, a CG bead-spring model combined with BD was used in Ref. [258] to show dependency of liquid – liquid phase separation and self-assembly regions of silk-like block-proteins dependency on the protein length, see Figure 6, which

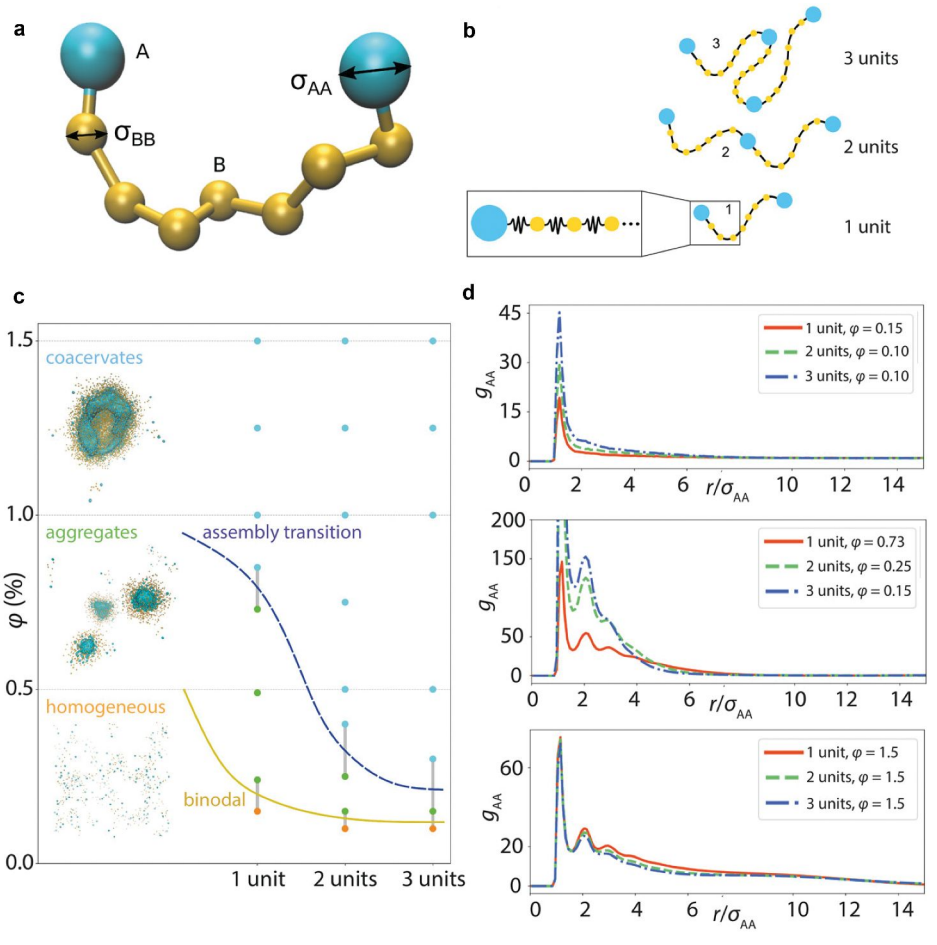

Figure 6. Example of BD simulations reach in the context of a bead-spring model for silk-like proteins of varying length (1 to 3 units) and their assembly phase behavior. a) Design and variables of the model. Bead types A and B differ by their diameter σ_{AA} and σ_{BB} and interactions. b) Silk-like proteins of 1 unit, 2 units, and 3 units were modelled. c) Resulting assembly phase diagram for the proteins at different volume fractions φ in the BD simulations. The visualizations show representative final simulation configurations for each of the assembly phases for the short 1 unit silk models. d) Structural analysis of the assemblies via radial distribution function $g_{AA}(r)$ calculated for the larger end beads A in the assemblies corresponding to different volume fractions. In Ref. [258], the BD simulations data aids interpreting the characterization data by experiments. Reprinted from Ref. [258] (CC by 4.0).

is presented to demonstrate that such simplified approach can extract protein length- and concentration-dependent transitions between distinct assembly morphologies.

Furthermore, BD approaches have mapped the charge or charged region dependency of polymers, such as RNA and some modular proteins. For example, based on BD simulations, a differentiation between non-specific binding interactions and localized charge interactions in protein assembly system has been identified, reporting that non-specific interactions have a larger effect

on liquid-liquid phase separation related droplet formation at lower protein-polymer interaction energies in the same system [259]. The BD procedure outlined in Ref. [260] focuses on investigating the dynamics and structural characteristics of protein solutions. This approach maintains atomistic details of the proteins while treating the solvent as a continuous medium. Notably, the modelling led to various quantities matching quantitatively experimental data and theoretical predictions benchmarking.

Also polymeric networks and effect of their cross-link density on their properties have been modelled by means of BD methods [261,262]. For protein hydrogels, the initial volume fraction was found as a dominant parameter to govern the assembly and its properties at the network level, but the characteristics of the single protein remain important [261]. Also the effects of changes in both the cross-link topology and flexibility of the polymeric building blocks have been mapped by BD approaches [262].

Reference [263] presents a rather interesting hybrid modelling approach to biopolymers. The implementation of mean field models of translational and rotational hydrodynamic interactions into an atomistically detailed many-protein BD simulation method is outlined [263]. The approach reveals the importance of both the solvent mediated and the weak protein-protein interactions for describing the dynamics and the assembly in concentrated protein solutions [263]. Further in this context, Ref. [264] introduces a framework in which generic amyloid forming proteins are represented by a single highly CG particle. The self-assembly of these CG particles into oligomers and fibrils was studied by means of BD simulations.

BD simulations have also been used to study the ejection dynamics of spherically confined active polymers through small pores, revealing that three stages, namely, a mainly entropy-driven, an active forces accelerated ejection process, and an active force dominated stage govern the ejection process [265]. Generalization to the applicability of particle-based BD dynamics techniques to model diffusive phenomena in biological environments is provided in the short review, Ref. [266], and revisited in Ref. [244].

6. Stochastic sampling approaches in particle-based modelling of biopolymers

So far, the surveyed particle-based approaches have relied on obtaining the time evolution of the system via numerical integration of equations of motion. For MD, the interactions governing the system were fully deterministic. In DPD, Langevin, or Brownian dynamics simulations, the approach contained also stochastic noise and dissipative contributions. Generally, modelling the response of the molecular system involved recursive integration of the resulting time-dependent differential equations for the positions, and in some

cases, velocities. Complementary to these, also approaches based on stochastic sampling of the possible states that the system can take exist. These are generally referred to as Monte Carlo (MC) simulations.

Mainly, MC methods rely on repeated random sampling to obtain numerical results. The most standard MC simulations approach in molecular modelling is the Metropolis MC method, in which the system states are sampled with outcome weights corresponding to the Boltzmann distribution, i.e. sampling the NVT ensemble [67]. The underlying interaction model is deterministic, and the measurable outcome is an expected value of the equilibrium. No kinetics information is included in the algorithm. However, other more advanced approaches exist, such as NpT MC and Grand Canonical MC that allow sampling also other statistical mechanics ensembles [67]. For example, the latter has been used to study ligand-protein binding [267]. Also kinetic MC, for capturing, as the name indicates, kinetics exists [67]. For a review of this approach, see e.g. Ref. [268]. MC methods are frequently implemented on a lattice, particularly in the context of polymeric systems. For books on MC simulations see e.g. Refs. [67,269].

MC approaches can be extremely powerful in polymer modelling due to the approach relying on stochastic sampling. Recent examples of MC studies of biopolymers include rather interesting CG approaches to protein amyloids, first developed for amyloid formation [270], later also for oligomer dynamics during amyloid fibril formation [271], and to reveal pathways of amyloid aggregation on cell membranes [272], as well as aggregation of fibril-forming proteins in the presence of interfaces [273]. In Ref. [272], the membrane-assisted nucleation of proteins that is relevant for understanding general macromolecular aggregation on lipid membranes was examined. The topic rises broad interest in both biological and biotechnological context. Assuming two distinct conformations for the proteins, namely a soluble and a β-sheet-prone conformation, the results revealed that the properties of the lipid membranes, such as membrane fluidity and protein-membrane affinity, result in fundamentally different morphologies and compositions of the aggregates, but also their nucleation pathways for protein aggregate formation exist, see Figure 7 for details.

Liquid-liquid phase separation and protein phase separation in general have received significant attention also by MC approaches [249,274,275]. Monte Carlo approaches have also found their use in studying protein systems with anisotropic, patchy interactions [276–278]. Another interesting direction is the hybrid method incorporating molecular-level MC simulations into single chain in mean-field simulations [279]. The work links molecular structure with the large-scale morphological features of polymer self-assembly.

MC modelling of biopolymers has also uncovered the interactions underlying the phase behaviour and properties of *Caenorhabditis elegans* protein

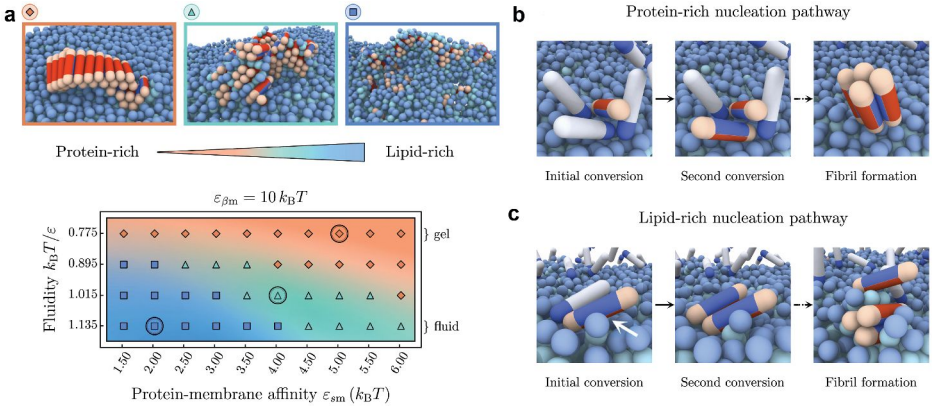

Figure 7. Example of reach of MC type approaches to CG proteins modelling. In the model, the CG proteins in the soluble state are white with a blue end and the β-sheet-prone conformation is presented by red and blue patches and pale ends. a) The model reveals assembly phases of the protein–lipid cluster morphologies depending on the membrane fluidity and protein–membrane affinity. Three main areas can be distinguished: extended fibrils (orange), smaller fibrillar clusters with interstitial lipids (green), and strongly mixed lipid–protein clusters (blue). The representative snapshots correspond to the circled parameter values; soluble proteins are not shown. b) Series of simulation visualization snapshots showing the gel-phase heterogeneous nucleation pathway resulting in protein-rich fibrillar clusters where the membrane acts as a static surface. c) Initial nucleation step in the fluid-phase nucleation pathway is caused by direct contact between the protein side patch and lipid tails (white arrow), typically leading to mixed lipid–protein aggregates. Reprinted from Ref. [272].

LAF-1 droplets by combining fluorescence correlation spectroscopy with a theoretical framework and insights from all-atom MC simulations [280]. Furthermore, the kinetics of poly-L-lysine adsorption on silica have been addressed by a combination of experiments and CG MC simulations, following the random sequential adsorption scheme [281]. Finally, MC approaches are also powerful in biopolymer structure prediction [282,283].

7. Field theory approaches in modelling of biopolymers

Beyond particle-based approaches, field theory methods to polymer materials allow describing polymer solutions and assemblies, including multicomponent mixtures, in a variety of settings and applications. They reach mesoscale and continuum level structure formation, and allow the study of, e.g., polymer material flows and reorganization at large scale, however omitting molecular level structure and largely the particle-like characteristics of the molecules. Here, we cover briefly first self-consistent field theory (SCFT), and after that classical density functional theory (cDFT), both for polymers. Whereas for SCFT multiple broad reviews already exist, cDFT which has comparable performance power in polymer modelling is less known.

Self-consistent field theory approaches

SCFT for polymers, initially developed in Ref. [284], is a successful, functional-based CG mean-field theory. The major approximation of the approach is that the monomers of a polymer chain are assumed to have a Gaussian spatial distribution. Reference [69] provides an in-depth overview of the technique, discussing the approximations and the available extensions to, e.g., polymer brushes, homopolymer interfaces, and block copolymer microstructures. More recently, SCFT approaches have been used to study also more complex macromolecules, such as, e.g., dendrimers [285], ring polymers [286], star copolymers [287], and complex processes such as liquid – liquid phase separation during amphiphilic self-assembly [288].

SCFT has proven to be of high practical use in predicting polymer materials response. This also reflects on its wide practical applications in biopolymer modelling. SCFT for polymeric materials, along with its usability and prediction ability for large scale assembly response, has been solidly established, see e.g. Ref. [289]. As the approach is field-theory based, and considers spatial distributions, the thoroughly reviewed polymer modelling approaches, e.g., Refs. [69,290,291], remain valid also for biopolymers. Research examples highlighting especially the biopolymer aspect include, e.g., polysaccharide modelling [292,293], polysaccharide-protein mixtures [294] and amyloids [295].

Classical (dynamical) density functional theory

Like SCFT, also cDFT is a means to study structure formation and assembly, but also dynamical reorganization in polymeric systems. Also pattern formation and component segregation can be readily mapped in length and time scales corresponding to both mesoscale and continuum levels. cDFT relies on expressing the governing thermodynamic potential, which, depending on the appropriate statistical ensemble, takes the form of either the free energy of the system (NVT ensemble), or the grand canonical potential energy (μVT ensemble), as a density dependent functional (i.e. a function of a function), which is then minimized as a function of the latter to resolve the system response in terms of density distribution [296–298].

Let us consider the cDFT formulation in the grand canonical ensemble. The grand canonical potential Ω can be expressed as a function of the Helmholtz free energy $\mathcal{F}$

$$\Omega[\rho(\mathbf{r})] = \mathcal{F}[\rho(\mathbf{r})] + \int d\mathbf{r}\,[V^{\text{ext}}(\mathbf{r}) - \mu]\,\rho(\mathbf{r}), \tag{16}$$

where μ is the (fixed) chemical potential and $V^{\text{ext}}(\mathbf{r})$ the external potential. Note that in bulk $V^{\text{ext}}(\mathbf{r}) \equiv 0$. By definition, the equilibrium average density profile $\rho_0(\mathbf{r})$ minimises Eq. 16. Therefore, the equilibrium density also satisfies the Euler-Lagrange equation

$$\left.\frac{\delta\Omega[\rho(\mathbf{r})]}{\delta\rho(\mathbf{r})}\right|_{\rho_0(\mathbf{r})} = 0. \tag{17}$$

Note that $\frac{\delta\Omega[\rho]}{\delta\rho}$ is a functional derivative [299] rather than a standard derivative. $\mathcal{F}$ is generally written as

$$\mathcal{F}[\rho(\mathbf{r})] = \mathcal{F}^{\text{id}}[\rho(\mathbf{r})] + \mathcal{F}^{\text{exc}}[\rho(\mathbf{r})], \tag{18}$$

where the first term is the ideal gas contribution, having the known form [299]

$$\mathcal{F}^{\text{id}}[\rho(\mathbf{r})] = k_{\text{B}}T \int d\mathbf{r}\rho(\mathbf{r})\left[\ln\left(\Lambda^d\rho(\mathbf{r})\right) - 1\right]. \tag{19}$$

In this, Λ is the thermal de Broglie wavelength and d the dimensionality of the system. The second term in Eq. 18 is the excess Helmholtz free energy functional, which models the interactions between particles, and takes different forms depending on the system at hand. For example, at the highest CG level, the interaction potential between pairs of particles representing polymeric systems are often designed using the generalized exponential model of index n (GEM-n), namely $\phi(r) = \varepsilon \exp[-(r/R)^n]$, see e.g. Refs. [300–306]. In this, ε controls the repulsion strength and R is a measure of the radius (of gyration) of the molecules. Most common choices for the exponent are $n = 2, 4, 8$. Here, and also more generally for ultra-soft interaction potentials, the excess free energy functional is often expressed in the mean field form, i.e. by convoluting the local density with the interaction potential ϕ [302,307–311]. This leads to

$$\mathcal{F}^{\text{exc}}[\rho(\mathbf{r})] = \int d\mathbf{r}d\mathbf{r}'\rho(\mathbf{r})\rho(\mathbf{r}')\phi(|\mathbf{r} - \mathbf{r}'|). \tag{20}$$

If more accurate approximations are needed, for example the so-called hypernetted chain Ornstein-Zernike integral equation theory can be used [299]. For an exhaustive and general review on cDFT, not focused on such highly coarse-grained polymers, but rather on its theoretical developments, see Ref. [312].

Because of the effective character of the interactions between the modelled species, the chemical specificity of the studied systems is usually lost. Nevertheless, cDFT can be exploited to provide general understanding on phenomena such as phase separation, transport, and self-assembly, at scales that are not reachable by more detailed approaches. For example, the key intermolecular interaction features responsible for complex self-assembling structures in binary mixtures of polymers have been identified [311]. This work also demonstrate how the assembly and species mixing can be controlled, providing insight in controlling polymeric and protein-based materials.

Furthermore, the key principles behind the emergence of structures with competing length scales in soft matter systems, including polymeric systems, have been addressed in Ref. [313], by means of both cDFT and DPD simulations. Furthermore, crystallization response of CG model dendrimers or star polymers under different confinements has been addressed in Ref. [314]. For related polymeric systems, a rich phase behavior consisting in two crystalline phases, a fluid phase, as well as metastable quasicrystal structures, has been found [309,315]. The employed CG model represents, e.g., dendrimers in which the inner generations of monomers are one type (e.g. hydrophobic), while the outer generations are another type (e.g. hydrophilic).

To obtain dynamics based on the cDFT formalism, one can resort to integration of the Smoluchowski equation [316,317] over all but one particle coordinates. This yields an exact expression for the time dependency of the average one-body density profile $\rho(\mathbf{r}, t)$ [298] in the form of a continuity equation $\partial_t \rho(\mathbf{r}, t) = -\nabla \mathbf{j}(\mathbf{r}, t)$, where ∂_t denotes the time derivative, and where the flux $\mathbf{j}$ involves an integral of the non-equilibrium two-body density $\rho^{(2)}(\mathbf{r}, \mathbf{r}', t)$. By invoking the adiabatic approximation on the two-body density [318], which corresponds to assuming that the non-equilibrium correlations are the same as in an equilibrium system, the continuity equation above provides the common advected form of the classical dynamical DFT (cDDFT) [319], reading

$$\frac{\partial \rho(\mathbf{r}, t)}{\partial t} + \nabla \cdot (\rho(\mathbf{r}, t)\mathbf{v}_s(\mathbf{r}, t)) = \frac{1}{\gamma} \nabla \cdot \left[\rho(\mathbf{r}, t) \nabla \frac{\delta F[\rho(\mathbf{r}, t)]}{\delta \rho(\mathbf{r}, t)} \right]. \tag{21}$$

For a full derivation of Eq. 21, see e.g. Refs. [320,321]. In the latter equation, $\mathbf{v}_s(\mathbf{r}, t)$ is the solvent velocity, $F[\rho(\mathbf{r}, t)] = \mathcal{F}[\rho(\mathbf{r}, t)] + \int V^{\text{ext}}(\mathbf{r}) \rho(\mathbf{r}, t) d\mathbf{r}$ is the total Helmholtz free energy functional from equilibrium cDFT [297,299], and γ the friction coefficient. In this framework, model potentials of the GEM-n class [322,323], but also more complex and multi-length-scales interaction potentials [324], have been used to study rheological response of CG polymeric systems under different external flows. In the latter, the interplay between external shear deformation and the characteristic length-scales

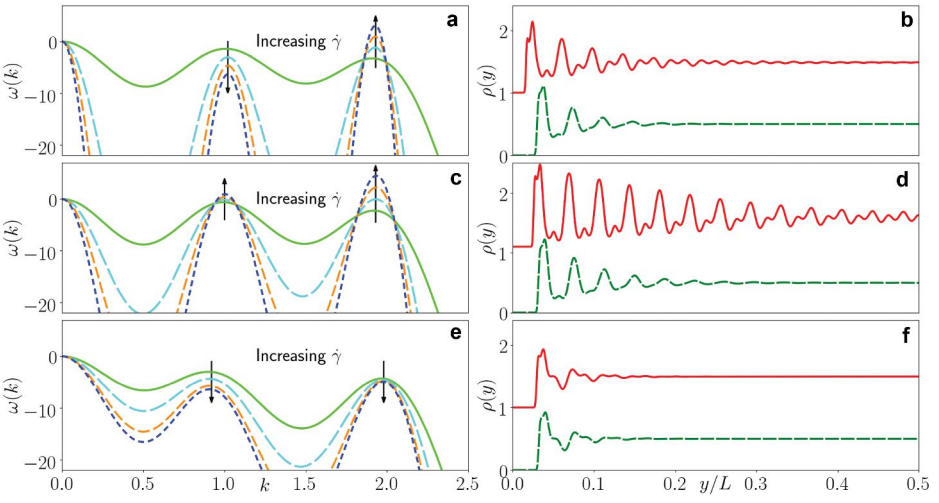

Figure 8. Demonstration of modelling reach of the cDDFT approach in the context of modelling CG polymeric systems under shear in a channel of width L. At left, linear dispersion relation $\omega(k)$ for varying shear rate $\dot{\gamma}$. The solid line corresponds to the unsheared $\dot{\gamma} = 0$ case. Increasing $\dot{\gamma}$ is indicated by the long dashed, intermediate dashed, and short dashed lines, respectively. At right, the corresponding density profiles from cDDFT calculations across the channel. Here, the dashed line is for $\dot{\gamma} = 0$ (unsheared equilibrium system) and the solid line is the steady state for a particular $\dot{\gamma}>0$ (data of panels b) and f) is vertically shifted by 1, and data of panel d) by 1.1). Three cases with slightly different interaction potentials are considered, for details see Figure 1 of Ref. [324]. The top row (panels a) and b)) shows a case in which as $\dot{\gamma}$ is increased, the first peak at $k \approx 1$ decreases, while the second at $k \approx 2$ increases. For sufficiently strong shear above a critical value, ($\dot{\gamma}>\dot{\gamma}_c$), one can eventually swap from one dominant length-scale to the other. Panel b) shows that shearing the suspension makes the short (wavelength) length-scale more prominent and the long length-scale less so. The middle row (panels c) and d)) shows that as $\dot{\gamma}$ is increased, both peaks in $\omega(k)$ increase in value, leading eventually to the system becoming linearly unstable. Panel d) shows that shear makes both length-scales more prominent and they have a slower decay away from the wall compared to the unsheared case. The short length-scale (almost not visible for $\dot{\gamma} = 0$) becomes slightly dominant. The bottom row (panels e) and f)) shows a case in which increase of $\dot{\gamma}$ moves both peaks in $\omega(k)$ down, making all density modulations even more strongly damped, so decreasing any structuring away from the wall. The corresponding density profiles are in panel f). Reprinted from Ref. [324] (CC by 4.0).

in the interparticle correlations of a soft-particles model system (such as polymers or assemblies of polymers) was examined, showing that shear can tune the characteristic length-scale from one to another quite distinct value [324]. Specific small changes in the form of the particle pair interactions led to external shear selectively enhance or suppress the different characteristic wavelengths of the system [324]. Figure 8 illustrates this by means of the linear dispersion relation and the average density profiles across the channel in which the soft particles are suspended, with and without external shear.

For GEM-n particles, also the solidification fronts under quench from the liquid state have been addressed [325]. cDDFT has also been applied to study the adsorption kinetics of globular proteins onto charged core – shell microgel particles, and the findings have been successfully tested on lysozyme

adsorption on PNIPAM coated nanoparticles [326]. Furthermore, the self-assembly behavior of the sphere-forming di-block copolymers confined in the square well was addressed systematically [327]. In a similar spirit, cDDFT was used to map morphologies of tri-block copolymers induced by cylindrical nanopores [328], demonstrating the approach for predicting assembly morphology changes. Reference [310], motivated by heterogeneous domain structure on the surface of cells, considers a minimal model consisting of a binary mixture of GEM-2 particles to study the dynamics of phase separation on the surface of a sphere. A different dynamical response depending on the relative size of the considered spheres, further scrutinized in Ref. [329] by means of power spectrum and the Minkowski functionals, was reported.

For more complex extensions of cDDFT than presented here, and their applications, see the extensive review by te Vrugt et al. [330]. Future perspective is provided in Ref. [331].

8. Summary

Biopolymers provide an excellent replacement for their synthetic, often fossil fuel-based counterparts [332]. They are a biodegradable and biocompatible substitute that holds the promise to address many environmental concerns and to reduce long-term man-made damages on a variety of ecosystems [8,9]. These also provide a staple for developing materials with advanced functionalities [7,9,333]. Furthermore, biopolymers are in key role in many biological processes. Both cellular functions and many pathogenic functions, for example many neurodegenerative diseases, rise from assembly and folding responses of specific proteins [334,335]. Regardless of applications purpose or natural environment in which the biopolymers function, theoretical models provide an easily up-scaled, effective means to examine the chemical dependencies of biopolymer on structural properties, assembly response, interactions, and dynamics. In these approaches, one can readily change a single variable at the time to predict the response of the system at hand, in contrast with many experiments, where the complexity of the system makes this task very arduous.

In this review, we discussed a variety of modelling approaches that have been or can be used for biopolymers. Notably, polymeric materials are multiscale by nature and thus different levels of description are required to tackle these systems, often combined together to different extents , see e.g. Ref. [41]. Hence, both chemically specific approaches, as well as highly CG techniques were covered. We focused on providing an overview of physics-based biopolymer modelling approaches employed for tackling current biopolymer materials modelling challenges, but due to the close relation to some materials directions, some examples rise from biological systems. Specifically, we focused on particle-based simulations methods, including all-atom

and CG MD, DPD, Langevin and BD approaches, as well as brief overview on stochastic sampling approaches (MC methods), and free energy functional based methods, such as SCFT, and c(D)DFT. In addition to these, a large variety of other theoretical models that can be applied to biopolymers exist. We omitted here, e.g., Lattice Boltzmann approaches [336], Markov Chains [337,338], and the classical polymer physics originating scaling approaches, but also a number of combination approaches bridging scales in polymer modelling [339].

Generally, the more chemically specific the model is, the more microscopic information on the biopolymers can be obtained. Moving into larger length and time scales reach, the connection with specific polymers is lost to an increasing degree. Nevertheless, the large-scale predictions by these methods capture a vast collection of polymers and assembly responses, as well as, dynamics. However, it is also evident that modelling accuracy at all scales, as well as bridging the different scales in modelling, remain the pressing challenges – the development required is both technical and at the level of how the existing physics-based approaches are best combined with each other, but also with the fast rising data-based approaches [59,60,340].

We point that also two additional and recent reviews in the field exists. The first is a thorough review on CG models targeted on studying the formation and biological function of macromolecular assemblies in living organisms [341], whereas the second provides a topical review on multiscale modelling of silk and silk-based biomaterials [342]. Finally, the reader might also find interest in Ref. [343], where the synthesis, structure, assembly, properties, and applications of protein-based block copolymers are thoroughly reviewed.

Funding

This work was supported by the Academy of Finland through project no. [359180] (M.S.) and its Centres of Excellence Programme (2022-2029, LIBER) under project no. [346111] (M.S.), by the Novo Nordisk Foundation under project no. [NNF22OC0074060] (M.S.) and [NNF22OC0079084] (A.S.), and by the Swiss National Science Foundation under the project no. [P500PT_206916] (A.S.).

Disclosure statement

No potential conflict of interest was reported by the author(s).

Author contributors

All authors participated in designing the concept of the article and in material collection. M.V. wrote the first draft of Sections 1–4 and A.S. of Sections 5–8. All authors contributed to reviewing and editing of the final manuscript. M.S. instructed the work.

ORCID

A. Scacchi http://orcid.org/0000-0003-4606-5400
M. Vuorte http://orcid.org/0000-0001-9652-8608
M. Sammalkorpi http://orcid.org/0000-0002-9248-430X

References

[1] Meraldo A. Introduction to bio-based polymers. In: John RW, editor. Multilayer flexible packaging. 2nd ed. Norwich (NY), USA: William Andrew Publishing; 2016. p. 47–52. doi: 10.1016/B978-0-323-37100-1.00004-1.
[2] George A, Sanjay MR, Srisuk R, et al. A comprehensive review on chemical properties and applications of biopolymers and their composites. Int J Biol Macromol. 2020;154:329–338. doi: 10.1016/j.ijbiomac.2020.03.120
[3] Liu C, Luan P, Li Q, et al. Biopolymers derived from trees as sustainable multifunctional materials: a review. Adv Mater. 2021;33(28):2001654. doi: 10.1002/adma.202001654
[4] Hatti-Kaul R, Nilsson LJ, Zhang B, et al. Designing biobased recyclable polymers for plastics. Trends Biotechnol. 2020;38(1):50–67. doi: 10.1016/j.tibtech.2019.04.011
[5] Mahmoud Zaghloul MY, Yousry Zaghloul MM, Yousry Zaghloul MM. Developments in polyester composite materials – an in-depth review on natural fibres and nano fillers. Compos Struct. 2021;278:114698. doi: 10.1016/j.compstruct.2021.114698
[6] Mtibe A, Motloung MP, Bandyopadhyay J, et al. Synthetic Biopolymers and Their Composites: Advantages and Limitations—An Overview. Macromol Rapid Commun. 2021;42(15):2100130. doi: 10.1002/marc.202100130
[7] Chen PY, McKittrick J, Meyers MA. Biological materials: functional adaptations and bioinspired designs. Pro Mater Sci. 2012;57(8):1492–1704. doi: 10.1016/j.pmatsci.2012.03.001
[8] Iwata T. Biodegradable and bio-based polymers: future prospects of eco-friendly plastics. Angew Chem Int Ed. 2015;54(11):3210–3215. doi: 10.1002/anie.201410770
[9] Kabir E, Kaur R, Lee J, et al. Prospects of biopolymer technology as an alternative option for non-degradable plastics and sustainable management of plastic wastes. J Clean Prod. 2020;258:120536. doi: 10.1016/j.jclepro.2020.120536
[10] Andrady AL, Neal MA. Applications and societal benefits of plastics. Philos Trans R Soc B. 2009;364(1526):1977–1984. doi: 10.1098/rstb.2008.0304
[11] Hale RC, Seeley ME, La Guardia MJ, et al. A global perspective on microplastics. J Geophys Res Oceans. 2020;125(1):e2018JC014719. doi: 10.1029/2018JC014719
[12] MacLeod M, Arp HPH, Tekman MB, et al. The global threat from plastic pollution. Science. 2021;373(6550):61–65. doi: 10.1126/science.abg5433
[13] Lebreton L, Andrady A. Future scenarios of global plastic waste generation and disposal. Palgrave Commun. 2019;5(1):1–11. doi: 10.1057/s41599-018-0212-7
[14] Borrelle SB, Ringma J, Law KL, et al. Predicted growth in plastic waste exceeds efforts to mitigate plastic pollution. Science. 2020;369(6510):1515–1518. doi: 10.1126/science.aba3656
[15] Gough CR, Callaway K, Spencer E, et al. Biopolymer-based filtration materials. ACS Omega. 2021;6(8):11804–11812. doi: 10.1021/acsomega.1c00791
[16] Khwaldia K, Arab-Tehrany E, Desobry S. Biopolymer coatings on paper packaging materials. Compr Rev Food Sci Food Saf. 2010;9(1):82–91. doi: 10.1111/j.1541-4337.2009.00095.x
[17] Tang X, Kumar P, Alavi S, et al. Recent advances in biopolymers and biopolymer-based nanocomposites for food packaging materials. Crit Rev Food Sci Nutr. 2012;52(5):426–442. doi: 10.1080/10408398.2010.500508

[18] Pinto L, Bonifacio MA, De Giglio E, et al. Biopolymer hybrid materials: Development, characterization, and food packaging applications. Food Pack Shelf Life. 2021;28:100676. doi: 10.1016/j.fpsl.2021.100676
[19] Khalid MY, Arif ZU. Novel biopolymer-based sustainable composites for food packaging applications: A narrative review. Food Pack Shelf Life. 2022;33:100892. doi: 10.1016/j.fpsl.2022.100892
[20] Papuc C, Goran GV, Predescu CN, et al. Plant polyphenols as antioxidant and antibacterial agents for shelf-life extension of meat and meat products: classification, structures, sources, and action mechanisms. Compr Rev Food Sci Food Saf. 2017;16(6):1243–1268. doi: 10.1111/1541-4337.12298
[21] Gharsallaoui A, Joly C, Oulahal N, et al. Nisin as a food preservative: part 2: antimicrobial polymer materials containing nisin. Crit Rev Food Sci Nutr. 2016;56(8):1275–1289. doi: 10.1080/10408398.2013.763766
[22] Li J, Yu X, Martinez EE, et al. Emerging biopolymer-based bioadhesives. Macromol biosci. 2022;22(2):2100340. doi: 10.1002/mabi.202100340
[23] Park SB, Lih E, Park KS, et al. Biopolymer-based functional composites for medical applications. Progress Polym Sci. 2017;68:77–105. doi: 10.1016/j.progpolymsci.2016.12.003
[24] Sahana T, Rekha P. Biopolymers: Applications in wound healing and skin tissue engineering. Mol Biol Rep. 2018;45(6):2857–2867. doi: 10.1007/s11033-018-4296-3
[25] Rebelo R, Fernandes M, Fangueiro R. Biopolymers in medical implants: A brief review. Procedia Eng. 2017;200:236–243. doi: 10.1016/j.proeng.2017.07.034
[26] Banerjee A, Ganguly S. Alginate–chitosan composite hydrogel film with macrovoids in the inner layer for biomedical applications. J Appl Polym Sci. 2019;136(22):47599. doi: 10.1002/app.47599
[27] Hu X, Cebe P, Weiss AS, et al. Protein-based composite materials. Mater Today. 2012;15(5):208–215. doi: 10.1016/S1369-7021(12)70091-3
[28] De La Rica R, Matsui H. Applications of peptide and protein-based materials in bionanotechnology. Chem Soc Rev. 2010;39(9):3499–3509. doi: 10.1039/b917574c
[29] Spicer CD, Jumeaux C, Gupta B, et al. Peptide and protein nanoparticle conjugates: versatile platforms for biomedical applications. Chem Soc Rev. 2018;47(10):3574–3620. doi: 10.1039/C7CS00877E
[30] Devadas VV, Khoo KS, Chia WY, et al. Algae biopolymer towards sustainable circular economy. Biores Technol. 2021;325:124702. doi: 10.1016/j.biortech.2021.124702
[31] Kuska J, O'Reilly E. Engineered biosynthetic pathways and biocatalytic cascades for sustainable synthesis. Curr Opin Chem Biol. 2020;58:146–154. doi: 10.1016/j.cbpa.2020.08.006
[32] Cao M, Tran VG, Zhao H. Unlocking nature's biosynthetic potential by directed genome evolution. Curr Opinion Biotechnol. 2020;66:95–104. Tissue, Cell and Pathway Engineering. doi: 10.1016/j.copbio.2020.06.012
[33] Fernando IS, Kim D, Nah JW, et al. Advances in functionalizing fucoidans and alginates (bio) polymers by structural modifications: A review. Chem Eng J. 2019;355:33–48. doi: 10.1016/j.cej.2018.08.115
[34] Shadish JA, DeForest CA. Site-selective protein modification: From functionalized proteins to functional biomaterials. Matter. 2020;2(1):50–77. doi: 10.1016/j.matt.2019.11.011
[35] Negm NA, Hefni HH, Abd-Elaal AA, et al. Advancement on modification of chitosan biopolymer and its potential applications. Int J Biol Macromol. 2020;152:681–702. doi: 10.1016/j.ijbiomac.2020.02.196

[36] Blanco Parte FG, Santoso SP, Chou CC, et al. Current progress on the production, modification, and applications of bacterial cellulose. Cri Rev Biotechnol. 2020;40(3):397–414. doi: 10.1080/07388551.2020.1713721
[37] Polman EM, Gruter GJM, Parsons JR, et al. Comparison of the aerobic biodegradation of biopolymers and the corresponding bioplastics: A review. Sci Total Environ. 2021;753:141953. doi: 10.1016/j.scitotenv.2020.141953
[38] Ling S, Kaplan D, Buehler M. Nanofibrils in nature and materials engineering. Nature Rev Mater. 2018;3:18016. doi: 10.1038/natrevmats.2018.16
[39] Burla F, Mulla Y, Vos BE, et al. From mechanical resilience to active material properties in biopolymer networks. Nat Rev Phys. 2019;1:249–263. doi: 10.1038/s42254-019-0036-4
[40] Lorenz C, Köster S. Multiscale architecture: Mechanics of composite cytoskeletal networks. Biophys Rev. 2022 08;3(3):031304. doi: 10.1063/5.0099405
[41] Schmid F. Understanding and modeling polymers: The challenge of multiple scales. ACS Polym Au. 2023;3(1):28–58. doi: 10.1021/acspolymersau.2c00049
[42] Heckert M, Kállay M, Tew DP, et al. Basis-set extrapolation techniques for the accurate calculation of molecular equilibrium geometries using coupled-cluster theory. J Chem Phys. 2006;125(4). doi: 10.1063/1.2217732
[43] Puzzarini C. Astronomical complex organic molecules: quantum chemistry meets rotational spectroscopy. Int J Quantum Chem. 2017;117(2):129–138. doi: 10.1002/qua.25284
[44] Puzzarini C. Accurate molecular structures of small-and medium-sized molecules. Int J Quantum Chem. 2016;116(21):1513–1519. doi: 10.1002/qua.25202
[45] Pinto SMV, Tasinato N, Barone V, et al. Modeling amino-acid side chain infrared spectra: the case of carboxylic residues. Phys Chem Chem Phys. 2020;22(5):3008–3016. doi: 10.1039/C9CP04774C
[46] Dudev T, Lim C. All-electron calculations of the nucleation structures in metal-induced zinc-finger folding: role of the peptide backbone. J Am Chem Soc. 2007;129(41):12497–12504. doi: 10.1021/ja073322c
[47] Culka M, Rulíšek L. Factors stabilizing β-sheets in protein structures from a quantum-chemical perspective. J Phys Chem B. 2019;123(30):6453–6461. doi: 10.1021/acs.jpcb.9b04866
[48] Culka M, Galgonek J, Vym etal J, et al. Toward Ab initio protein folding: Inherent secondary structure propensity of short peptides from the bioinformatics and quantum-chemical perspective. J Phys Chem B. 2019;123(6):1215–1227. doi: 10.1021/acs.jpcb.8b09245
[49] Perez A, Morrone JA, Simmerling C, et al. Advances in free-energy-based simulations of protein folding and ligand binding. Curr Opinion Struct Biol. 2016;36:25–31. doi: 10.1016/j.sbi.2015.12.002
[50] Dhahagani K, Kesavan MP, Vinoth KGG, et al. Crystal structure, optical properties, DFT analysis of new morpholine based Schiff base ligands and their copper (II) complexes: DNA, protein docking analyses, antibacterial study and anticancer evaluation. Mater Sci Eng C. 2018;90:119–130. doi: 10.1016/j.msec.2018.04.032
[51] Choubey SK, Prabhu D, Nachiappan M, et al. Molecular modeling, dynamics studies and density functional theory approaches to identify potential inhibitors of SIRT4 protein from Homo sapiens: a novel target for the treatment of type 2 diabetes. J Biomol Struct Dynamics. 2017;35(15):3316–3329. doi: 10.1080/07391102.2016.1254117
[52] Šponer J, Šponer JE, Mládek A, et al. Nature and magnitude of aromatic base stacking in DNA and RNA: quantum chemistry, molecular mechanics, and experiment. Biopolymers. 2013;99(12):978–988. doi: 10.1002/bip.22322

[53] Chandramouli B, Del Galdo S, Mancini G, et al. Tailor-made computational protocols for precise characterization of small biological building blocks using QM and MM approaches. Biopolymers. 2018;109(10):e23109. doi: 10.1002/bip.23109
[54] Vennelakanti V, Nazemi A, Mehmood R, et al. Harder, better, faster, stronger: Large-scale QM and QM/MM for predictive modeling in enzymes and proteins. Curr Opinion Struct Biol. 2022;72:9–17. doi: 10.1016/j.sbi.2021.07.004
[55] Liu J, He X. Fragment-based quantum mechanical approach to biomolecules, molecular clusters, molecular crystals and liquids. Phys Chem Chem Phys. 2020;22(22):12341–12367. doi: 10.1039/D0CP01095B
[56] Yilmazer ND, Korth M. Enhanced semiempirical QM methods for biomolecular interactions. Computat Struct Biotechnol J. 2015;13:169–175. doi: 10.1016/j.csbj.2015.02.004
[57] Van der Spoel D. Systematic design of biomolecular force fields. Curr Opinion Struct Biol. 2021;67:18–24. doi: 10.1016/j.sbi.2020.08.006
[58] Huggins DJ, Biggin PC, Dämgen MA, et al. Biomolecular simulations: From dynamics and mechanisms to computational assays of biological activity. Wiley Interdiscip Rev Comput Mol Sci. 2019;9(3):e1393. doi: 10.1002/wcms.1393
[59] Butler KT, Davies DW, Cartwright H, et al. Machine learning for molecular and materials science. Nature. 2018;559:547–555. doi: 10.1038/s41586-018-0337-2
[60] Himanen L, Geurts A, Foster AS, et al. Data-driven materials science: status, challenges, and perspectives. Adv Sci. 2019;6(21):1900808. doi: 10.1002/advs.201900808
[61] Zhang Y, He H, Liu Y, et al. Recent progress in theoretical and computational studies on the utilization of lignocellulosic materials. Green Chem. 2019;21:9–35. doi: 10.1039/C8GC02059K
[62] Mehandzhiyski AY, Zozoulenko I. A review of cellulose coarse-grained models and their applications. Polysaccharides. 2021;2(2):257–270. doi: 10.3390/polysaccharides2020018
[63] Zhou S, Jin K, Buehler MJ. Understanding plant biomass via computational modeling. Adv Mater. 2021;33(28):2003206. doi: 10.1002/adma.202003206
[64] Wohlert M, Benselfelt T, Gberg L W, et al. Cellulose and the role of hydrogen bonds: Not in charge of everything. Cellul. 2022;29:1–23. doi: 10.1007/s10570-021-04325-4
[65] Guseva Aal DV, K Glagolev M, Vasilevskaya VV. Revealing structural and physical properties of polylactide: What simulation can do beyond the experimental methods. Polymer Rev. 2023;64:1–39. doi: 10.1080/15583724.2023.2174136
[66] Kotla NG, Pandey A, Vijaya Kumar Y, et al. Polyester-based long acting injectables: advancements in molecular dynamics simulation and technological insights. Drug Discovery Today. 2023;28(2):103463. doi: 10.1016/j.drudis.2022.103463
[67] Frenkel D, Smit B. Understanding molecular simulation: from algorithms to applications. 3rd ed. USA: Academic Press; 2023. doi: 10.1016/C2009-0-63921-0
[68] Allen MP, Tildesley DJ. Computer Simulation of Liquids. Oxford (UK): Oxford University Press; 2017. doi: 10.1093/oso/9780198803195.001.0001
[69] Matsen MW. Self-consistent field theory and its applications. Gompper G, and Schick M, editors. Soft Matter. 1, Polymer Melts and Mixtures. Darmstadt, Germany: Wiley-VCH;2005. p. 1–84. doi: 10.1002/9783527617050.ch2
[70] Gogonea V, Suárez D, van der Vaart A, et al. New developments in applying quantum mechanics to proteins. Curr Opinion Struct Biol. 2001;11(2):217–223. doi: 10.1016/S0959-440X(00)00193-7
[71] Giese B, Graber M, Cordes M. Electron transfer in peptides and proteins. Curr Opin Chem Biol. 2008;12(6):755–759. doi: 10.1016/j.cbpa.2008.08.026

[72] Chung LW, Sameera W, Ramozzi R, et al. The ONIOM method and its applications. Chem Rev. 2015;115(12):5678–5796. doi: 10.1021/cr5004419
[73] Lambert N, Chen YN, Cheng YC, et al. Quantum biology. Nat Phys. 2013;9(1):10–18. doi: 10.1038/nphys2474
[74] Merz KM Jr. Using quantum mechanical approaches to study biological systems. Acc Chem Res. 2014;47(9):2804–2811. doi: 10.1021/ar5001023
[75] Zhao G, Perilla JR, Yufenyuy EL, et al. Mature HIV-1 capsid structure by cryo-electron microscopy and all-atom molecular dynamics. Nature. 2013;497(7451):643–646. doi: 10.1038/nature12162
[76] Yu I, Mori T, Ando T, et al. Biomolecular interactions modulate macromolecular structure and dynamics in atomistic model of a bacterial cytoplasm. eLife. 2016;5:e19274. doi: 10.7554/eLife.19274
[77] Jung J, Nishima W, Daniels M, et al. Scaling molecular dynamics beyond 100,000 processor cores for large-scale biophysical simulations. J Comput Chem. 2019;40(21):1919–1930. doi: 10.1002/jcc.25840
[78] Hollingsworth SA, Dror RO. Molecular dynamics simulation for all. Neuron. 2018;99(6):1129–1143. doi: 10.1016/j.neuron.2018.08.011
[79] Rapaport DC. The art of molecular dynamics simulation. 2nd ed. Cambridge, United Kingdom: Cambridge University Press; 2004. doi: 10.1017/CBO9780511816581
[80] Fröhlking T, Bernetti M, Calonaci N, et al. Toward empirical force fields that match experimental observables. J Chem Phys. 2020 06;152(23)230902. doi: 10.1063/5.0011346
[81] Lopes PE, Guvench O, MacKerell AD. Current status of protein force fields for molecular dynamics simulations. In Kukoi A, editor. Molecular Modelling of Proteins. 215, Methods in Molecular Biology. New York, NY: Humana Press; 2015. p. 47–71. doi: 10.1007/978-1-4939-1465-4_3
[82] van Gunsteren WF, Daura X, Hansen N, et al. Validation of molecular simulation: An overview of issues. Angew Chem Int Ed. 2018;57(4):884–902. doi: 10.1002/anie.201702945
[83] Bottaro S, Lindorff-Larsen K. Biophysical experiments and biomolecular simulations: A perfect match? Science. 2018;361(6400):355–360. doi: 10.1126/science.aat4010
[84] Pierce LC, Salomon-Ferrer R, de Oliveira AF, et al. Routine access to millisecond time scale events with accelerated molecular dynamics. J Chem Theory Comput. 2012;8(9):2997–3002. doi: 10.1021/ct300284c
[85] Kutzner C, Páll S, Fechner M, et al. Best bang for your buck: GPU nodes for GROMACS biomolecular simulations. J Comput Chem. 2015;36(26):1990–2008. doi: 10.1002/jcc.24030
[86] Bernardi RC, Melo MC, Schulten K. Enhanced sampling techniques in molecular dynamics simulations of biological systems. Biochim Biophys Acta. 2015;1850:872–877. doi: 10.1016/j.bbagen.2014.10.019
[87] Huang J, MacKerell AD Jr. Force field development and simulations of intrinsically disordered proteins. Curr Opinion Struct Biol. 2018;48:40–48. doi: 10.1016/j.sbi.2017.10.008
[88] Jing Z, Liu C, Cheng SY, et al. Polarizable force fields for biomolecular simulations: Recent advances and applications. Annu Rev Biophys. 2019;48:371. doi: 10.1146/annurev-biophys-070317-033349
[89] Lemkul JA, Huang J, MacKerell AD Jr. Induced dipole–dipole interactions influence the unfolding pathways of wild-type and mutant amyloid β-peptides. J Phys Chem B. 2015;119(51):15574–15582. doi: 10.1021/acs.jpcb.5b09978

[90] Lemkul JA, Huang J, Roux B, et al. An empirical polarizable force field based on the classical Drude oscillator model: development history and recent applications. Chem Rev. 2016;116(9):4983–5013. doi: 10.1021/acs.chemrev.5b00505
[91] Radak BK, Chipot C, Suh D, et al. Constant-pH molecular dynamics simulations for large biomolecular systems. J Chem Theory Comput. 2017;13(12):5933–5944. doi: 10.1021/acs.jctc.7b00875
[92] Dobrev P, Vemulapalli SPB, Nath N, et al. Probing the accuracy of explicit solvent constant pH molecular dynamics simulations for peptides. J Chem Theory Comput. 2020;16(4):2561–2569. doi: 10.1021/acs.jctc.9b01232
[93] Buslaev P, Aho N, Jansen A, et al. Best practices in constant pH MD simulations: Accuracy and sampling. J Chem Theory Comput. 2022;18(10):6134–6147. doi: 10.1021/acs.jctc.2c00517
[94] Aho N, Buslaev P, Jansen A, et al. Scalable constant pH molecular dynamics in GROMACS. J Chem Theory Comput. 2022;18(10):6148–6160. doi: 10.1021/acs.jctc.2c00516
[95] Goh GB, Hulbert BS, Zhou H, et al. Constant pH molecular dynamics of proteins in explicit solvent with proton tautomerism. Proteins. 2014;82(7):1319–1331. doi: 10.1002/prot.24499
[96] Dobrev P, Donnini S, Groenhof G, et al. Accurate three states model for amino acids with two chemically coupled titrating sites in explicit solvent atomistic constant pH simulations and pKa calculations. J Chem Theory Comput. 2017;13(1):147–160. doi: 10.1021/acs.jctc.6b00807
[97] Grimsley GR, Scholtz JM, Pace CN. A summary of the measured pK values of the ionizable groups in folded proteins. Protein Sci. 2009;18:247–251. doi: 10.1002/pro.19
[98] Inakollu VS, Geerke DP, Rowley CN, et al. Polarisable force fields: What do they add in biomolecular simulations? Curr Opinion Struct Biol. 2020;61:182–190. doi: 10.1016/j.sbi.2019.12.012
[99] Zhu Q, Ge Y, Li W, et al. Treating polarization effects in charged and polar bio-molecules through variable electrostatic Parameters. J Chem Theory Comput. 2023;19(2):396–411. doi: 10.1021/acs.jctc.2c01130
[100] Rauscher S, Gapsys V, Gajda MJ, et al. Structural ensembles of intrinsically disordered proteins depend strongly on force field: A comparison to experiment. J Chem Theory Comput. 2015;11:5513–5524. doi: 10.1021/acs.jctc.5b00736
[101] Huang J, Rauscher S, Nawrocki G, et al. CHARMM36m: an improved force field for folded and intrinsically disordered proteins. Nat Methods. 2017;14:71–73. doi: 10.1038/nmeth.4067
[102] Robustelli P, Piana S, Shaw DE. Developing a molecular dynamics force field for both folded and disordered protein states. Proc Natl Acad Sci, USA. 2018;115(21):E4758–66. doi: 10.1073/pnas.1800690115
[103] Mu J, Liu H, Zhang J, et al. Recent force field strategies for intrinsically disordered proteins. J Chem Inf Model. 2021;61(3):1037–1047. doi: 10.1021/acs.jcim.0c01175
[104] Yoo J, Aksimentiev A. New tricks for old dogs: improving the accuracy of biomolecular force fields by pair-specific corrections to non-bonded interactions. Phys Chem Chem Phys. 2018;20(13):8432–8449. doi: 10.1039/C7CP08185E
[105] Dans PD, Ivani I, Hospital A, et al. How accurate are accurate force-fields for B-DNA? Nucleic Acids Res. 2017 01;45(7):4217–4230. doi: 10.1093/nar/gkw1355
[106] Salsbury AM, Lemkul JA. Recent developments in empirical atomistic force fields for nucleic acids and applications to studies of folding and dynamics. Curr Opinion Struct Biol. 2021;67:9–17. doi: 10.1016/j.sbi.2020.08.003

[107] Tucker MR, Piana S, Tan D, et al. Development of force field parameters for the simulation of single- and double-stranded DNA molecules and DNA–protein complexes. J Phys Chem B. 2022;126(24):4442–4457. doi: 10.1021/acs.jpcb.1c10971
[108] Batys P, Morga M, Bonarek P, et al. pH-induced changes in Polypeptide conformation: force-field comparison with experimental validation. J Phys Chem B. 2020;124(14):2961–2972. doi: 10.1021/acs.jpcb.0c01475
[109] Wang A, Peng X, Li Y, et al. Quality of force fields and sampling methods in simulating pepX peptides: a case study for intrinsically disordered proteins. Phys Chem Chem Phys. 2021;23:2430–2437. doi: 10.1039/D0CP05484D
[110] Hamid MK, Månsson LK, Meklesh V, et al. Molecular dynamics simulations of the adsorption of an intrinsically disordered protein: Force field and water model evaluation in comparison with experiments. Front Mol Biosci. 2022;9. doi: 10.3389/fmolb.2022.958175
[111] Tolmachev DA, Boyko OS, Lukasheva NV, et al. Overbinding and qualitative and quantitative changes caused by simple Na+ and K+ ions in polyelectrolyte simulations: Comparison of force fields with and without NBFIX and ECC corrections. J Chem Theory Comput. 2020;16(1):677–687. doi: 10.1021/acs.jctc.9b00813
[112] Lukasheva N, Tolmachev D, Martinez-Seara H, et al. Changes in the local conformational states caused by simple Na+ and K+ ions in polyelectrolyte simulations: comparison of seven force fields with and without NBFIX and ECC corrections. Polymers. 2022;14(2):252. doi: 10.3390/polym14020252
[113] Cranford SW, Tarakanova A, Pugno NM, et al. Nonlinear material behaviour of spider silk yields robust webs. Nature. 2012;482(7383):72–76. doi: 10.1038/nature10739
[114] Giesa T, Perry CC, Buehler MJ. Secondary structure transition and critical stress for a model of spider silk assembly. Biomacromolecules. 2016;17(2):427–436. doi: 10.1021/acs.biomac.5b01246
[115] Batys P, Fedorov D, Mohammadi P, et al. Self-assembly of silk-like protein into nanoscale bicontinuous networks under phase-separation conditions. Biomacromolecules. 2021;22(2):690–700. doi: 10.1021/acs.biomac.0c01506
[116] Tolmachev DA, Malkamäki M, Linder MB, et al. Spidroins under the influence of alcohol: Effect of ethanol on secondary structure and molecular level solvation of silk-like proteins. Biomacromolecules. 2023;24(12):5638–5653. doi: 10.1021/acs.biomac.3c00637
[117] Li NK, Quiroz FG, Hall CK, et al. Molecular description of the LCST behavior of an elastin-like polypeptide. Biomacromolecules. 2014;15(10):3522–3530. doi: 10.1021/bm500658w
[118] Condon JE, Martin TB, Jayaraman A. Effect of conjugation on phase transitions in thermoresponsive polymers: an atomistic and coarse-grained simulation study. Soft Matter. 2017;13(16):2907–2918. doi: 10.1039/C6SM02874H
[119] Tarakanova A, Huang W, Qin Z, et al. Modeling and experiment reveal structure and nanomechanics across the inverse temperature transition in B. mori silk-elastin-like protein polymers. ACS Biomater Sci Eng. 2017;3(11):2889–2899. doi: 10.1021/acsbiomaterials.6b00688
[120] Prhashanna A, Taylor PA, Qin J, et al. Effect of peptide sequence on the LCST-like transition of elastin-like peptides and elastin-like peptide–collagen-like peptide conjugates: Simulations and experiments. Biomacromolecules. 2019;20(3):1178–1189. doi: 10.1021/acs.biomac.8b01503
[121] Gautieri A, Vesentini S, Redaelli A, et al. Hierarchical structure and nanomechanics of collagen microfibrils from the atomistic scale up. Nano Lett. 2011;11(2):757–766. doi: 10.1021/nl103943u

[122] Nair A, Gautieri A, Chang SW, et al. Molecular mechanics of mineralized collagen fibrils in bone. Nano Lett. 2013;4:1724. doi: 10.1038/ncomms2720
[123] Milazzo M, David A, Jung GS, et al. Molecular origin of viscoelasticity in mineralized collagen fibrils. Biomater Sci. 2021;9:3390–3400. doi: 10.1039/D0BM02003F
[124] Tolmachev D, Lukasheva N, Mamistvalov G, et al. Influence of calcium binding on conformations and motions of anionic polyamino acids. Effect of side chain length. Polymers. 2020;12(6):1279. doi: 10.3390/polym12061279
[125] Tolmachev D, Mamistvalov G, Lukasheva N, et al. Effects of amino acid side-chain length and chemical structure on anionic polyglutamic and polyaspartic acid cellulose-based polyelectrolyte brushes. Polymers. 2021;13(11):1789. doi: 10.3390/polym13111789
[126] Harmat AL, Morga M, Lutkenhaus JL, et al. Molecular mechanisms of pH-tunable stability and surface coverage of polypeptide films. Appl Surface Sci. 2023;615:156331. doi: 10.1016/j.apsusc.2023.156331
[127] Milazzo M, Jung GS, Danti S, et al. Wave propagation and energy dissipation in collagen molecules. ACS Biomater Sci Eng. 2020;6(3):1367–1374. doi: 10.1021/acsbiomaterials.9b01742
[128] Emami FS, Puddu V, Berry RJ, et al. Prediction of specific biomolecule adsorption on silica surfaces as a function of pH and particle size. Chem Mater. 2014;26(19):5725–5734. doi: 10.1021/cm5026987
[129] Patwardhan SV, Emami FS, Berry RJ, et al. Chemistry of aqueous silica nanoparticle surfaces and the mechanism of selective peptide adsorption. J Am Chem Soc. 2012;134(14):6244–6256. doi: 10.1021/ja211307u
[130] Ghobadi AF, Jayaraman A. Effects of polymer conjugation on hybridization thermodynamics of oligonucleic acids. J Phys Chem B. 2016;120(36):9788–9799. doi: 10.1021/acs.jpcb.6b06970
[131] Schneider J, Colombi Ciacchi L. Specific material recognition by small peptides mediated by the interfacial solvent structure. J Am Chem Soc. 2012;134(4):2407–2413. doi: 10.1021/ja210744g
[132] Qin Z, Buehler MJ. Molecular mechanics of mussel adhesion proteins. J Mech Phys Solids. 2014;62:19–30. doi: 10.1016/j.jmps.2013.08.015
[133] Rakkapao N, Vao-Soongnern V. Molecular simulation and experimental studies of the miscibility of chitosan/poly (ethylene oxide) blends. J Polym Res. 2014;21(12):1–10. doi: 10.1007/s10965-014-0606-1
[134] Liwo A, Czaplewski C, Sieradzan AK, etal. Chapter Two - Scale-consistent approach to the derivation of coarse-grained force fields for simulating structure, dynamics, and thermodynamics of biopolymers. In: Strodel B, and Barz B, editors. Computational approaches for understanding dynamical systems: protein folding and assembly. Vol. 170, Progress in Molecular Biology and Translational Science. Cambridge, MA, United States: Academic Press; 2020. p. 73–122. doi: 10.1016/bs.pmbts.2019.12.004
[135] Li J, Chen SJ. RNA 3D structure prediction using coarse-grained models. Front Mol Biosci. 2021;8:8. doi: 10.3389/fmolb.2021.720937
[136] Kmiecik S, Gront D, Kolinski M, et al. Coarse-grained protein models and their applications. Chem Rev. 2016;116(14):7898–7936. doi: 10.1021/acs.chemrev.6b00163
[137] Brini E, Algaer EA, Ganguly P, et al. Systematic coarse-graining methods for soft matter simulations – a review. Soft Matter. 2013;9:2108–2119. doi: 10.1039/C2SM27201F
[138] Jin J, Pak AJ, Durumeric AE, et al. Bottom-up coarse-graining: Principles and perspectives. J Chem Theory Comput. 2022;18(10):5759–5791. doi: 10.1021/acs.jctc.2c00643

[139] Arnarez C, Uusitalo JJ, Masman MF, et al. Dry Martini, a coarse-grained force field for lipid membrane simulations with implicit solvent. J Chem Theory Comput. 2015;11(1):260–275. doi: 10.1021/ct500477k
[140] Marrink SJ, Corradi V, Souza PC, et al. Computational modeling of realistic cell membranes. Chem Rev. 2019;119(9):6184–6226. doi: 10.1021/acs.chemrev.8b00460
[141] Dhamankar S, Webb MA. Chemically specific coarse-graining of polymers: methods and prospects. J Polym Sci. 2021;59(22):2613–2643. doi: 10.1002/pol.20210555
[142] Potter TD, Tasche J, Wilson MR. Assessing the transferability of common top-down and bottom-up coarse-grained molecular models for molecular mixtures. Phys Chem Chem Phys. 2019;21:1912–1927. doi: 10.1039/C8CP05889J
[143] Jarin Z, Newhouse J, Voth GA. Coarse-Grained Force Fields from the Perspective of Statistical Mechanics: Better Understanding of the Origins of a MARTINI Hangover. J Chem Theory Comput. 2021;17(2):1170–1180. doi: 10.1021/acs.jctc.0c00638
[144] Liwo A, Baranowski M, Czaplewski C, et al. A unified coarse-grained model of biological macromolecules based on mean-field multipole–multipole interactions. J Mol Model. 2014;20(8):1–15. doi: 10.1007/s00894-014-2306-5
[145] Vierros S, Sammalkorpi M. Hybrid atomistic and coarse-grained Model for surfactants in apolar solvents. ACS Omega. 2019;4(13):15581–15592. doi: 10.1021/acsomega.9b01959
[146] Souza PC, Alessandri R, Barnoud J, et al. Martini 3: A general purpose force field for coarse-grained molecular dynamics. Nat Methods. 2021;18(4):382–388. doi: 10.1038/s41592-021-01098-3
[147] Marrink SJ, De Vries AH, Mark AE. Coarse grained model for semiquantitative lipid simulations. J Phys Chem B. 2004;108(2):750–760. doi: 10.1021/jp036508g
[148] Marrink SJ, Risselada HJ, Yefimov S, et al. The MARTINI force field: coarse grained model for biomolecular simulations. J Phys Chem B. 2007;111(27):7812–7824. doi: 10.1021/jp071097f
[149] López CA, Sovova Z, van Eerden FJ, et al. Martini force field parameters for glycolipids. J Chem Theory Comput. 2013;9(3):1694–1708. doi: 10.1021/ct3009655
[150] Uusitalo JJ, Ingólfsson HI, Akhshi P, et al. Martini coarse-grained force field: Extension to DNA. J Chem Theory Comput. 2015;11(8):3932–3945. doi: 10.1021/acs.jctc.5b00286
[151] Uusitalo JJ, Ingólfsson HI, Marrink SJ, et al. Martini coarse-grained force field: extension to RNA. Biophys J. 2017;113(2):246–256. doi: 10.1016/j.bpj.2017.05.043
[152] López CA, Rzepiela AJ, de Vries AH, et al. Martini coarse-grained force field: Extension to carbohydrates. J Chem Theory Comput. 2009;5(12):3195–3210. doi: 10.1021/ct900313w
[153] López CA, Bellesia G, Redondo A, et al. MARTINI coarse-grained model for crystalline cellulose microfibers. J Phys Chem B. 2015;119(2):465–473. doi: 10.1021/jp5105938
[154] Schmalhorst PS, Deluweit F, Scherrers R, et al. Overcoming the limitations of the MARTINI force field in simulations of polysaccharides. J Chem Theory Comput. 2017;13(10):5039–5053. doi: 10.1021/acs.jctc.7b00374
[155] Shivgan AT, Marzinek JK, Huber RG, et al. Extending the Martini coarse-grained force field to N-Glycans. J Chem Inf Model. 2020;60(8):3864–3883. doi: 10.1021/acs.jcim.0c00495
[156] Lutsyk V, Wolski P, Plazinski W. Extending the Martini 3 coarse-grained force field to carbohydrates. J Chem Theory Comput. 2022;18:5089–5107. doi: 10.1021/acs.jctc.2c00553
[157] Grünewald F, Punt MH, Jefferys EE, et al. Martini 3 coarse-grained force field for carbohydrates. J Chem Theory Comput. 2022;18(8):7555–7569. doi: 10.1021/acs.jctc.2c00757

[158] Pang J, Mehandzhiyski AY, Zozoulenko I. Martini 3 model of surface modified cellulose nanocrystals: investigation of aqueous colloidal stability. Cellul. 2022;29(18):9493–9509. doi: 10.1007/s10570-022-04863-5
[159] Rossi G, Monticelli L, Puisto SR, et al. Coarse-graining polymers with the MARTINI force-field: polystyrene as a benchmark case. Soft Matter. 2011;7(2):698–708. doi: 10.1039/C0SM00481B
[160] Nawaz S, Carbone P. Coarse-graining poly (ethylene oxide)–poly (propylene oxide)–poly (ethylene oxide)(PEO–PPO–PEO) block copolymers using the MARTINI force field. J Phys Chem B. 2014;118(6):1648–1659. doi: 10.1021/jp4092249
[161] Panizon E, Bochicchio D, Monticelli L, et al. MARTINI coarse-grained models of polyethylene and polypropylene. J Phys Chem B. 2015;119(25):8209–8216. doi: 10.1021/acs.jpcb.5b03611
[162] Banerjee P, Roy S, Nair N. Coarse-grained molecular dynamics force-field for polyacrylamide in infinite dilution derived from iterative Boltzmann inversion and MARTINI force-field. J Phys Chem B. 2018;122(4):1516–1524. doi: 10.1021/acs.jpcb.7b09019
[163] Dans PD, Zeida A, Machado MR, et al. A coarse grained model for atomic-detailed DNA simulations with explicit electrostatics. J Chem Theory Comput. 2010;6(5):1711–1725. doi: 10.1021/ct900653p
[164] Darré L, Machado MR, Brandner AF, et al. SIRAH: A structurally unbiased coarse-grained force field for proteins with aqueous solvation and long-range electrostatics. J Chem Theory Comput. 2015;11(2):723–739. doi: 10.1021/ct5007746
[165] Machado MR, Barrera EE, Klein F, et al. The SIRAH 2.0 force field: Altius, fortius, citius. J Chem Theory Comput. 2019;15(4):2719–2733. doi: 10.1021/acs.jctc.9b00006
[166] Brandner A, Schüller A, Melo F, et al. Exploring DNA dynamics within oligonucleosomes with coarse-grained simulations: SIRAH force field extension for protein-DNA complexes. Biochem Biophys Res Commun. 2018;498(2):319–326. doi: 10.1016/j.bbrc.2017.09.086
[167] Dawid AE, Gront D, Kolinski A. SURPASS low-resolution coarse-grained protein modeling. J Chem Theory Comput. 2017;13(11):5766–5779. doi: 10.1021/acs.jctc.7b00642
[168] Gopal SM, Mukherjee S, Cheng YM, et al. PRIMO/PRIMONA: a coarse-grained model for proteins and nucleic acids that preserves near-atomistic accuracy. Proteins Struct Funct Bioinf. 2010;78(5):1266–1281. doi: 10.1002/prot.22645
[169] Kar P, Gopal SM, Cheng YM, et al. Transferring the PRIMO coarse-grained force field to the membrane environment: Simulations of membrane proteins and helix–helix association. J Chem Theory Comput. 2014;10(8):3459–3472. doi: 10.1021/ct500443v
[170] Noid WG. Perspective: coarse-grained models for biomolecular systems. J Chem Phys. 2013;139(9):09B201_1. doi: 10.1063/1.4818908
[171] Chen Y, Krämer A, Charron NE, et al. Machine learning implicit solvation for molecular dynamics. J Chem Phys. 2021;155(8):084101. doi: 10.1063/5.0059915
[172] Wang J, Charron N, Husic B, et al. Multi-body effects in a coarse-grained protein force field. J Chem Phys. 2021;154:164113. doi: 10.1063/5.0041022
[173] Durumeric AE, Charron NE, Templeton C, et al. Machine learned coarse-grained protein force-fields: Are we there yet? Curr Opinion Struct Biol. 2023;79:102533. doi: 10.1016/j.sbi.2023.102533
[174] Unke OT, Chmiela S, Sauceda HE, et al. Machine learning force fields. Chem Rev. 2021;121(16):10142–10186. doi: 10.1021/acs.chemrev.0c01111
[175] Zimmermann MT, Leelananda SP, Gniewek P, et al. Free energies for coarse-grained proteins by integrating multibody statistical contact potentials with entropies from elastic network models. J Struct Functional Genomics. 2011;12(2):137–147. doi: 10.1007/s10969-011-9113-3

[176] Gniewek P, Leelananda SP, Kolinski A, et al. Multibody coarse-grained potentials for native structure recognition and quality assessment of protein models. Proteins: Structure. Funct Bioinformat. 2011;79(6):1923–1929. doi: 10.1002/prot.23015
[177] Darre L, Tek A, Baaden M, et al. Mixing atomistic and coarse grain solvation models for MD simulations: Let WT4 handle the bulk. J Chem Theory Comput. 2012;8(10):3880–3894. doi: 10.1021/ct3001816
[178] Han W, Schulten K. Further optimization of a hybrid united-atom and coarse-grained force field for folding simulations: Improved backbone hydration and interactions between charged side chains. J Chem Theory Comput. 2012;8(11):4413–4424. doi: 10.1021/ct300696c
[179] Zavadlav J, Melo MN, Marrink SJ, et al. Adaptive resolution simulation of an atomistic protein in MARTINI water. J Chem Phys. 2014;140(5):054114. doi: 10.1063/1.4863329
[180] Kar P, Feig M. Hybrid all-atom/coarse-grained simulations of proteins by direct coupling of CHARMM and PRIMO force fields. J Chem Theory Comput. 2017;13(11):5753–5765. doi: 10.1021/acs.jctc.7b00840
[181] Ghobadi AF, Jayaraman A. Effect of backbone chemistry on hybridization thermodynamics of oligonucleic acids: a coarse-grained molecular dynamics simulation study. Soft Matter. 2016;12(8):2276–2287. doi: 10.1039/C5SM02868J
[182] Condon JE, Jayaraman A. Effect of oligonucleic acid (ONA) backbone features on assembly of ONA–star polymer conjugates: a coarse-grained molecular simulation study. Soft Matter. 2017;13(38):6770–6783. doi: 10.1039/C7SM01534H
[183] Malaspina DC, Szleifer I, Dhaher Y. Mechanical properties of a collagen fibril under simulated degradation. J Mech Behav Biomed Mater. 2017;75:549–557. doi: 10.1016/j.jmbbm.2017.08.020
[184] Chen CY, Escobedo FA. Molecular simulations of laser spike annealing of block copolymer lamellar thin-films. Langmuir. 2020;36(21):5754–5764. doi: 10.1021/acs.langmuir.0c00423
[185] Hyltegren K, Polimeni M, Skepö M, et al. Integrating All-Atom and Coarse-Grained Simulations—Toward Understanding of IDPs at Surfaces. J Chem Theory Comput. 2020;16(3):1843–1853. doi: 10.1021/acs.jctc.9b01041
[186] Hafner AE, Gyori NG, Bench CA, et al. Modeling fibrillogenesis of collagen-mimetic molecules. Biophys J. 2020;119(9):1791–1799. doi: 10.1016/j.bpj.2020.09.013
[187] Tarakanova A, Ozsvar J, Weiss AS, et al. Coarse-grained model of tropoelastin self-assembly into nascent fibrils. Mater Today Bio. 2019;3:3. doi: 10.1016/j.mtbio.2019.100016
[188] Vuorte M, Määttä J, Sammalkorpi M. Simulations study of single-component and mixed n-alkyl-PEG micelles. J Phys Chem B. 2018;122(18):4851–4860. doi: 10.1021/acs.jpcb.8b00398
[189] Viitala L, Pajari S, Gentile L, et al. Shape and phase transitions in a PEGylated phospholipid system. Langmuir. 2019;35(11):3999–4010. doi: 10.1021/acs.langmuir.8b03829
[190] Määttä J, Vierros S, Van Tassel PR, et al. Size-selective, noncovalent dispersion of carbon nanotubes by PEGylated lipids: a coarse-grained molecular dynamics study. J Chem Eng Data. 2014;59(10):3080–3089. doi: 10.1021/je500157b
[191] Lee H, Larson RG. Adsorption of plasma proteins onto PEGylated lipid bilayers: The effect of PEG size and grafting Density. Biomacromolecules. 2016;17(5):1757–1765. doi: 10.1021/acs.biomac.6b00146
[192] Davis LK, Šarić A, Hoogenboom BW, et al. Physical modeling of multivalent interactions in the nuclear pore complex. Biophys J. 2021;120(9):1565–1577. doi: 10.1016/j.bpj.2021.01.039

[193] Adamczyk Z. Modeling adsorption of colloids and proteins. Curr Opin Colloid Interface Sci. 2012;17(3):173–186. doi: 10.1016/j.cocis.2011.12.002
[194] Huertas J, Woods EJ, Collepardo-Guevara R. Multiscale modelling of chromatin organisation: Resolving nucleosomes at near-atomistic resolution inside genes. Curr Opinion Cell Biol. 2022;75:102067. doi: 10.1016/j.ceb.2022.02.001
[195] Tan C, Takada S. Nucleosome allostery in pioneer transcription factor binding. Proc Natl Acad Sci, USA. 2020;117(34):20586–20596. doi: 10.1073/pnas.2005500117
[196] Ding X, Lin X, Zhang B. Stability and folding pathways of tetra-nucleosome from six-dimensional free energy surface. Nat Commun. 2021;12(1):1091. doi: 10.1038/s41467-021-21377-z
[197] Alvarado W, Moller J, Ferguson AL, et al. Tetranucleosome interactions drive chromatin folding. ACS Central Sci. 2021;7(6):1019–1027. doi: 10.1021/acscentsci.1c00085
[198] Buitrago D, Labrador M, Arcon JP, et al. Impact of DNA methylation on 3D genome structure. Nat Commun. 2021;12(1):3243. doi: 10.1038/s41467-021-23142-8
[199] Sridhar A, Farr SE, Portella G, et al. Emergence of chromatin hierarchical loops from protein disorder and nucleosome asymmetry. Proc Natl Acad Sci, USA. 2020;117(13):7216–7224. doi: 10.1073/pnas.1910044117
[200] Farr SE, Woods EJ, Joseph JA, et al. Nucleosome plasticity is a critical element of chromatin liquid–liquid phase separation and multivalent nucleosome interactions. Nat Commun. 2021;12(1):2883. doi: 10.1038/s41467-021-23090-3
[201] Yang C, Chen X, Qiu H, et al. Dissipative particle dynamics simulation of phase behavior of aerosol OT/water system. J Phys Chem B. 2006;110(43):21735–21740. doi: 10.1021/jp0623692
[202] Espanol P, Warren PB. Perspective: dissipative particle dynamics. J Chem Phys. 2017;146(15):150901. doi: 10.1063/1.4979514
[203] Forrest BM, Suter UW. Accelerated equilibration of polymer melts by time-coarse-graining. J Chem Phys. 1995;102(18):7256–7266. doi: 10.1063/1.469037
[204] Groot RD, Warren PB. Dissipative particle dynamics: bridging the gap between atomistic and mesoscopic simulation. J Chem Phys. 1997;107(11):4423–4435. doi: 10.1063/1.474784
[205] Warner HR Jr. Kinetic theory and rheology of dilute suspensions of finitely extendible dumbbells. Ind Eng Chem Fundamentals. 1972;11(3):379–387. doi: 10.1021/i160043a017
[206] Español P. Fluid particle dynamics: a synthesis of dissipative particle dynamics and smoothed particle dynamics. EPL (Europhysics Letters). 1997;39(6):605. doi: 10.1209/epl/i1997-00401-5
[207] Warren P. Vapor-liquid coexistence in many-body dissipative particle dynamics. Phys Rev E. 2003;68(6):066702. doi: 10.1103/PhysRevE.68.066702
[208] Vaiwala R, Ayappa KG. A generic force field for simulating native protein structures using dissipative particle dynamics. Soft Matter. 2021;17:9772–9785. doi: 10.1039/D1SM01194D
[209] Vishnyakov A, Talaga DS, Neimark AV. DPD simulation of protein conformations: from α-helices to β-structures. J Phys Chem Lett. 2012;3(21):3081–3087. doi: 10.1021/jz301277b
[210] Mai Y, Eisenberg A. Self-assembly of block copolymers. Chem Soc Rev. 2012;41(18):5969–5985. doi: 10.1039/c2cs35115c
[211] Mai J, Sun D, Li L, et al. Phase behavior of an amphiphilic block copolymer in ionic liquid: a dissipative particle dynamics study. J Chem Eng Data. 2016;61(12):3998–4005. doi: 10.1021/acs.jced.6b00522

[212] Seki T, Arai N, Suh D, et al. Self-assembly of peptide amphiphiles by vapor pressure osmometry and dissipative particle dynamics. RSC Adv. 2018;8(47):26461–26468. doi: 10.1039/C8RA04692A

[213] Tokareva OS, Lin S, Jacobsen MM, et al. Effect of sequence features on assembly of spider silk block copolymers. J Struct Biol. 2014;186(3):412–419. doi: 10.1016/j.jsb.2014.03.004

[214] Lin S, Ryu S, Tokareva O, et al. Predictive modelling-based design and experiments for synthesis and spinning of bioinspired silk fibres. Nat Commun. 2015;6(1):1–12. doi: 10.1038/ncomms7892

[215] Liu LL, Yang ZZ, Zhao DX, et al. Morphological transition difference of linear and cyclic block copolymer with polymer blending in a selective solvent by combining dissipative particle dynamics and all-atom molecular dynamics simulations based on the ABEEM polarizable force field. RSC Adv. 2014;4(94):52083–52087. doi: 10.1039/C4RA09631B

[216] Javan Nikkhah S, Turunen E, Lepo A, et al. Multicore assemblies from three-component linear homo-copolymer systems: a coarse-grained modeling study. Polymers. 2021;13(13):2193. doi: 10.3390/polym13132193

[217] Javan Nikkhah S, Sammalkorpi M. Single core and multicore aggregates from a polymer mixture: A dissipative particle dynamics study. J Colloid Interface Sci. 2023;635:231–241. doi: 10.1016/j.jcis.2022.12.119

[218] Harmat AL, Javan Nikkhah S, Sammalkorpi M. Dissipative particle dynamics simulations of H-shaped diblock copolymer self-assembly in solvent. Polymer. 2021;233:124198. doi: 10.1016/j.polymer.2021.124198

[219] Javan Nikkhah S, Cazade PA, McManus JJ, et al. Design rules for antibody delivery by self-assembled block-copolyelectrolyte nanocapsules. Macromolecules. 2022;55(7):2383–2397. doi: 10.1021/acs.macromol.2c00118

[220] Javan Nikkhah S, Thompson D. Copolyelectrolyte-based nanocapsules for oral monoclonal antibody therapy: A mesoscale modeling survey. Biomacromolecules. 2022;23(9):3875–3886. doi: 10.1021/acs.biomac.2c00699

[221] Luo Z, Li Y, Wang B, et al. pH-sensitive vesicles formed by amphiphilic grafted copolymers with tunable membrane permeability for drug loading/release: a multiscale simulation study. Macromolecules. 2016;49(16):6084–6094. doi: 10.1021/acs.macromol.6b01211

[222] Terrón-Mejía KA, Martínez-Benavidez E, Higuera-Ciapara I, et al. Mesoscopic modeling of the encapsulation of capsaicin by lecithin/chitosan liposomal nanoparticles. Nanomaterials. 2018;8:425. doi: 10.3390/nano8060425

[223] Zhuang Z, Jiang T, Lin J, et al. Hierarchical nanowires synthesized by supramolecular stepwise polymerization. Angew Chem Int Ed. 2016;55(40):12522–12527. doi: 10.1002/anie.201607059

[224] Averick S, Karácsony O, Mohin J, et al. Cooperative, reversible self-assembly of covalently pre-linked proteins into giant fibrous structures. Angew Chem Int Ed. 2014;126(31):8188–8193. doi: 10.1002/ange.201402827

[225] Li Y, Zhang X, Cao D. The role of shape complementarity in the protein-protein interactions. Sci Rep. 2013;3(1):1–7. doi: 10.1038/srep03271

[226] Chen L, Jiang T, Lin J, et al. Toroid formation through self-assembly of graft copolymer and homopolymer mixtures: experimental studies and dissipative particle dynamics simulations. Langmuir. 2013;29(26):8417–8426. doi: 10.1021/la401553a

[227] Li X, Tang YH, Liang H, et al. Large-scale dissipative particle dynamics simulations of self-assembled amphiphilic systems. Chem Comm. 2014;50(61):8306–8308. doi: 10.1039/C4CC03096F

[228] Choudhury CK, Kuksenok O. Native-based dissipative particle dynamics approach for α-helical folding. J Phys Chem B. 2020;124(50):11379–11386. doi: 10.1021/acs.jpcb.0c08603
[229] Wang L, Tang Z, Li D, et al. Adsorption and ordering of amphiphilic rod–coil block copolymers on a substrate: Conditions for well-aligned stripe nanopatterns. Nanoscale. 2020;12(24):13119–13128. doi: 10.1039/D0NR01244K
[230] Shrivastava Ifra S, Saha S, Singh A. Dissipative particle dynamics simulation study on ATRP-brush modification of variably shaped surfaces and biopolymer adsorption. Phys Chem Chem Phys. 2022;24:17986–18003. doi: 10.1039/D2CP01749K
[231] Kobayashi Y, Nomura K, Kaneko T, et al. Replica exchange dissipative particle dynamics method on threadlike micellar aqueous solutions. J Phys. 2019;32(11):115901. doi: 10.1088/1361-648X/ab579c
[232] Posel Z, Svoboda M, Colina CM, et al. Flow and aggregation of rod-like proteins in slit and cylindrical pores coated with polymer brushes: an insight from dissipative particle dynamics. Soft Matter. 2017;13(8):1634–1645. doi: 10.1039/C6SM02751B
[233] Terrón-Mejía KA, López-Rendón R, Goicochea AG. Electrostatics in dissipative particle dynamics using Ewald sums with point charges. J Phys. 2016;28(42):425101. doi: 10.1088/0953-8984/28/42/425101
[234] Gavrilov AA, Chertovich AV, Kramarenko EY. Dissipative particle dynamics for systems with high density of charges: implementation of electrostatic interactions. J Chem Phys. 2016;145(17):174101. doi: 10.1063/1.4966149
[235] Peter EK, Lykov K, Pivkin IV. A polarizable coarse-grained protein model for dissipative particle dynamics. Phys Chem Chem Phys. 2015;17(37):24452–24461. doi: 10.1039/C5CP03479E
[236] Gavrilov AA. Dissipative particle dynamics for systems with polar species: interactions in dielectric media. J Chem Phys. 2020;152(16):164101. doi: 10.1063/5.0002475
[237] Gavrilov AA, Kramarenko EY. Two contributions to the dielectric response of polar liquids. J Chem Phys. 2021;154(11):116101. doi: 10.1063/5.0038440
[238] Mao R, Lee MT, Vishnyakov A, et al. Modeling aggregation of ionic surfactants using a smeared charge approximation in dissipative particle dynamics simulations. J Phys Chem B. 2015;119(35):11673–11683. doi: 10.1021/acs.jpcb.5b05630
[239] Peter EK, Pivkin IV. A polarizable coarse-grained water model for dissipative particle dynamics. J Chem Phys. 2014;141(16):10B613_1. doi: 10.1063/1.4899317
[240] Langevin P. On the theory of Brownian motion. Comptes Rendus de l'Académie des Sci (Paris). 1908;146:530.
[241] Coffey W, Kalmykov YP. The Langevin equation: with applications to stochastic problems in physics, chemistry and electrical engineering. 4th ed. Vol.28. World Scientific Series in Contemporary Chemical Physics. Hackensack, NJ, United States: World Scientific Pub Co. Inc.; 2017.
[242] Argun A, Callegari A, Volpe G. Brownian dynamics. In: Simulation of Complex Systems. 2053-2563. Bristol (UK): IOP Publishing; 2021. p. 5–1 to 5–13.
[243] Huber GA, McCammon JA. Brownian dynamics simulations of biological molecules. Trend Chem. 2019;1(8):727–738. doi: 10.1016/j.trechm.2019.07.008
[244] Muñiz-Chicharro A, Votapka LW, Amaro RE, et al. Brownian dynamics simulations of biomolecular diffusional association processes. WIREs Comput Mol Sci. 2023;13(3):e1649. doi: 10.1002/wcms.1649
[245] Kang H, Pincus PA, Hyeon C, et al. Effects of macromolecular crowding on the collapse of biopolymers. Phys Rev Lett. 2015;114(6):068303. doi: 10.1103/PhysRevLett.114.068303

[246] Di Cairano L, Stamm B, Calandrini V. Subdiffusive-Brownian crossover in membrane proteins: a generalized Langevin equation-based approach. Biophys J. 2021;120(21):4722–4737. doi: 10.1016/j.bpj.2021.09.033
[247] Smith WW, Ho PY, O'Hern CS. Calibrated Langevin-dynamics simulations of intrinsically disordered proteins. Phys Rev E. 2014;90(4):042709. doi: 10.1103/PhysRevE.90.042709
[248] Statt A, Casademunt H, Brangwynne CP, et al. Model for disordered proteins with strongly sequence-dependent liquid phase behavior. J Chem Phys. 2020;152(7). doi: 10.1063/1.5141095
[249] Shen C, Qin C, Tl X, et al. Structure and dynamics of an active polymer adsorbed on the surface of a cylinder. Soft Matter. 2022;18(7):1489–1497. doi: 10.1039/D1SM01658J
[250] Alapati S, Fernandes DV, Suh YK. Numerical simulation of the electrophoretic transport of a biopolymer through a synthetic nano-pore. Mol Simulat. 2011;37(06):466–477. doi: 10.1080/08927022.2011.553229
[251] Gong B, Lin J, Wei X, et al. Cross-linked biopolymer networks with active motors: Mechanical response and intra-network transport. J Mech Phys Solids. 2019;127:80–93. doi: 10.1016/j.jmps.2019.03.001
[252] Gong B, Wei X, Qian J, et al. Modeling and simulations of the dynamic behaviors of actin-based cytoskeletal networks. ACS Biomater Sci Eng. 2019;5(8):3720–3734. doi: 10.1021/acsbiomaterials.8b01228
[253] Walczak AM, Antosiewicz JM. Langevin dynamics of proteins at constant pH. Phys Rev E. 2002;66(5):051911. doi: 10.1103/PhysRevE.66.051911
[254] Brackley CA, Morozov AN, Marenduzzo D. Models for twistable elastic polymers in Brownian dynamics, and their implementation for LAMMPS. J Chem Phys. 2014;140(13):135103. doi: 10.1063/1.4870088
[255] Długosz M, Trylska J. Diffusion in crowded biological environments: Applications of Brownian dynamics. BMC Biophys. 2011;4:4. doi: 10.1186/2046-1682-4-3
[256] Smith S, Grima R. Fast simulation of Brownian dynamics in a crowded environment. J Chem Phys. 2017;146(2):024105. doi: 10.1063/1.4973606
[257] Blanco PM, Garcés JL, Madurga S, et al. Macromolecular diffusion in crowded media beyond the hard-sphere model. Soft Matter. 2018;14:3105–3114. doi: 10.1039/C8SM00201K
[258] Lemetti L, Scacchi A, Yin Y, et al. Liquid–liquid phase separation and assembly of silk-like proteins is dependent on the polymer length. Biomacromolecules. 2022;23:3142–3153. doi: 10.1021/acs.biomac.2c00179
[259] Zumbro E, Alexander-Katz A, Kudryavtsev YV. Multivalent polymers can control phase boundary, dynamics, and organization of liquid-liquid phase separation. PLOS ONE. 2021;16(11):e0245405. doi: 10.1371/journal.pone.0245405
[260] Mereghetti P, Gabdoulline RR, Wade RC. Brownian dynamics simulation of protein solutions: structural and dynamical properties. Biophys J. 2010;99(11):3782–3791. doi: 10.1016/j.bpj.2010.10.035
[261] Hanson BS, Dougan L. Network growth and structural characteristics of globular protein hydrogels. Macromolecules. 2020;53(17):7335–7345. doi: 10.1021/acs.macromol.0c00890
[262] Hanson BS, Dougan L. Intermediate structural hierarchy in biological networks modulates the fractal dimension and force distribution of percolating clusters. Biomacromolecules. 2021;22(10):4191–4198. doi: 10.1021/acs.biomac.1c00751
[263] Mereghetti P, Wade RC. Atomic detail Brownian dynamics simulations of concentrated protein solutions with a mean field treatment of hydrodynamic interactions. J Phys Chem B. 2012;116(29):8523–8533. doi: 10.1021/jp212532h

[264] Ilie IM, den Otter WK, Briels WJ. A coarse grained protein model with internal degrees of freedom. Application to α-synuclein aggregation. J Chem Phys. 2016;144(8):085103. doi: 10.1063/1.4942115
[265] Li C, Chen Z, Liu D, et al. Ejection dynamics of spherically confined active polymers through a small pore. Soft Matter. 2023;19(25):4628–4633. doi: 10.1039/D3SM00471F
[266] Długosz M, Trylska J. Diffusion in crowded biological environments: Applications of Brownian dynamics. BMC Biophys. 2011;4(1):1–9. doi: 10.1186/2046-1682-4-3
[267] Clark M, Guarnieri F, Shkurko I, et al. Grand canonical monte carlo simulation of ligand-protein binding. J Chem Inf Model. 2006;46(1):231–242. doi: 10.1021/ci050268f
[268] Andersen M, Panosetti C, Reuter K. A practical guide to surface kinetic Monte Carlo simulations. Front Chem. 2019;7:202. doi: 10.3389/fchem.2019.00202
[269] Landau D, Binder K. A guide to Monte Carlo simulations in statistical physics. Cambridge (UK): Cambridge University Press; 2021. doi: 10.1017/9781108780346
[270] Šarić A, Chebaro YC, Knowles TP, et al. Crucial role of nonspecific interactions in amyloid nucleation. Proc Natl Acad Sci, USA. 2014;111(50):17869–17874. doi: 10.1073/pnas.1410159111
[271] Michaels TC, Šarić A, Curk S, et al. Dynamics of oligomer populations formed during the aggregation of Alzheimer's Aβ42 peptide. Nat Chem. 2020;12(5):445–451. doi: 10.1038/s41557-020-0452-1
[272] Krausser J, Knowles TP, Šarić A. Physical mechanisms of amyloid nucleation on fluid membranes. Proc Natl Acad Sci, USA. 2020;117(52):33090–33098. doi: 10.1073/pnas.2007694117
[273] Toprakcioglu Z, Kamada A, Michaels TC, et al. Adsorption free energy predicts amyloid protein nucleation rates. Proc Natl Acad Sci, USA. 2022;119:e2109718119. doi: 10.1073/pnas.2109718119
[274] Das S, Eisen A, Lin YH, et al. A lattice model of charge-pattern-dependent polyampholyte phase separation. J Phys Chem B. 2018;122(21):5418–5431. doi: 10.1021/acs.jpcb.7b11723
[275] Rana U, Brangwynne CP, Panagiotopoulos AZ. Phase separation vs aggregation behavior for model disordered proteins. J Chem Phys. 2021;155(12):125101. doi: 10.1063/5.0060046
[276] Kurut A, Persson BA, Åkesson T, et al. Anisotropic interactions in protein mixtures: self assembly and phase behavior in aqueous solution. J Phys Chem Lett. 2012;3(6):731–734. doi: 10.1021/jz201680m
[277] Yigit C, Heyda J, Ballauff M, et al. Like-charged protein-polyelectrolyte complexation driven by charge patches. J Chem Phys. 2015;143(6):064905. doi: 10.1063/1.4928078
[278] Gnan N, Sciortino F, Zaccarelli E. Patchy particle models to understand protein phase behavior. In: McManus J, editor. Protein self-assembly. Methods in Molecular Biology. New York, NY: Humana; 2019. p. 187–208. doi: 10.1007/978-1-4939-9678-0_14
[279] Lytle TK, Radhakrishna M, Sing CE. High charge density coacervate assembly via hybrid Monte Carlo single chain in mean field theory. Macromolecules. 2016;49(24):9693–9705. doi: 10.1021/acs.macromol.6b02159
[280] Wei MT, Elbaum-Garfinkle S, Holehouse AS, et al. Phase behaviour of disordered proteins underlying low density and high permeability of liquid organelles. Nat Chem. 2017;9(11):1118–1125. doi: 10.1038/nchem.2803
[281] Kosior D, Morga M, Maroni P, et al. Formation of poly-l-lysine monolayers on silica: modeling and experimental studies. J Phys Chem C. 2020;124(8):4571–4581. doi: 10.1021/acs.jpcc.9b10870

[282] Boniecki MJ, Lach G, Dawson WK, et al. SimRNA: A coarse-grained method for RNA folding simulations and 3D structure prediction. Nucleic Acids Res. 2015 12;44(7):e63–3. doi: 10.1093/nar/gkv1479
[283] Watkins AM, Geniesse C, Kladwang W, et al. Blind prediction of noncanonical RNA structure at atomic accuracy. Sci Adv. 2018;4(5):eaar5316. doi: 10.1126/sciadv.aar5316
[284] Edwards SF. The statistical mechanics of polymers with excluded volume. Proc Phys Soc. 1965;85(4):613. doi: 10.1088/0370-1328/85/4/301
[285] Okrugin B, Neelov I, Leermakers F, et al. Structure of asymmetrical peptide dendrimers: Insights given by self-consistent field theory. Polymer. 2017;125:292–302. doi: 10.1016/j.polymer.2017.07.060
[286] Kim JU, Yang YB, Lee WB. Self-consistent field theory of Gaussian ring polymers. Macromolecules. 2012;45(7):3263–3269. doi: 10.1021/ma202583y
[287] Li W, Liu YX. Simplicity in mean-field phase behavior of two-component miktoarm star copolymers. J Chem Phys. 2021;154(1). doi: 10.1063/5.0037979
[288] Ianiro A, Wu H, van Rijt MM, et al. Liquid–liquid phase separation during amphiphilic self-assembly. Nat Chem. 2019;11(4):320–328. doi: 10.1038/s41557-019-0210-4
[289] Fredrickson GH, Ganesan V, Drolet F. Field-theoretic computer simulation methods for polymers and complex fluids. Macromolecules. 2002;35(1):16–39. doi: 10.1021/ma011515t
[290] Müller M, de Pablo JJ. Computational approaches for the dynamics of structure formation in self-assembling polymeric Materials. Ann Rev Mater Res. 2013;43(1):1–34. doi: 10.1146/annurev-matsci-071312-121618
[291] Müller M. Process-directed self-assembly of copolymers: Results of and challenges for simulation studies. Progress Polym Sci. 2020;101:101198. doi: 10.1016/j.progpolymsci.2019.101198
[292] Ettelaie R, Akinshina A, Maurer S. Mixed protein–polysaccharide interfacial layers: effect of polysaccharide charge distribution. Soft Matter. 2012;8(29):7582–7597. doi: 10.1039/c2sm25803j
[293] Ettelaie R, Akinshina A. Colloidal interactions induced by overlap of mixed protein+polysaccharide interfacial layers. Food Hydrocolloids. 2014;42:106–117. doi: 10.1016/j.foodhyd.2014.01.020
[294] Ettelaie R, Akinshina A, Dickinson E. Mixed protein–polysaccharide interfacial layers: A self consistent field calculation study. Faraday Disc. 2008;139:161–178. doi: 10.1039/b717199d
[295] van der Munnik NP, Sajib MSJ, Moss MA, et al. Determining the potential of mean force for amyloid-β dimerization: Combining self-consistent field theory with molecular dynamics simulation. J Chem Theory Comput. 2018;14(5):2696–2704. doi: 10.1021/acs.jctc.7b01057
[296] Evans R. The nature of the liquid-vapour interface and other topics in the statistical mechanics of non-uniform, classical fluids. Adv Phys. 1979;28(2):143–200. doi: 10.1080/00018737900101365
[297] Evans R. Density functionals in the theory of non-uniform Fluids. In Henderson D, editor. Fundamentals of Inhomogeneous Fluids. New York, (NY) USA: Marcel Dekker Inc; 1992; p. 85–176.
[298] Hansen JP, McDonald IR, editors. Theory of Simple Liquids. 4th ed. Oxford, (UK): Academic Press; 2013. doi: 10.1016/C2010-0-66723-X
[299] Gelfand IM, Fomin SV. Calculus of variations. English ed. Englewood Cliffs (NJ): Prentice-Hall, Inc; 1963.
[300] Bolhuis PG, Louis AA, Hansen JP, et al. Accurate effective pair potentials for polymer solutions. J Chem Phys. 2001;114(9):4296–4311. doi: 10.1063/1.1344606

[301] Likos CN. Effective interactions in soft condensed matter physics. Phys Rep. 2001;348(4–5):267–439. doi: 10.1016/S0370-1573(00)00141-1
[302] Archer AJ, Evans R. Binary Gaussian core model: fluid-fluid phase separation and interfacial properties. Phys Rev E. 2001;64(4):041501. doi: 10.1103/PhysRevE.64.041501
[303] Götze I, Harreis H, Likos CN. Tunable effective interactions between dendritic macromolecules. J Chem Phys. 2004;120(16):7761–7771. doi: 10.1063/1.1689292
[304] Likos CN. Soft matter with soft particles. Soft Matter. 2006;2(6):478–498. doi: 10.1039/b601916c
[305] Overduin S, Likos CN. Phase behaviour in binary mixtures of ultrasoft repulsive particles. Europhys Lett. 2009;85(2):26003. doi: 10.1209/0295-5075/85/26003
[306] van Teeffelen S, Moreno AJ, Likos CN. Cluster crystals in confinement. Soft Matter. 2009;5(5):1024–1038. doi: 10.1039/b813916d
[307] Louis A, Bolhuis P, Hansen J. Mean-field fluid behavior of the Gaussian core model. Phys Rev E. 2000;62(6):7961. doi: 10.1103/PhysRevE.62.7961
[308] Archer AJ, Likos CN, Evans R. Binary star-polymer solutions: bulk and interfacial properties. J Phys. 2002;14(46):12031. doi: 10.1088/0953-8984/14/46/311
[309] Archer AJ, Rucklidge AM, Knobloch E. Soft-core particles freezing to form a quasicrystal and a crystal-liquid phase. Phys Rev E. 2015;92(1):012324. doi: 10.1103/PhysRevE.92.012324
[310] Bott MC, Brader JM. Phase separation on the sphere: patchy particles and self-assembly. Phys Rev E. 2016;94(1):012603. doi: 10.1103/PhysRevE.94.012603
[311] Scacchi A, Sammalkorpi M, Ala-Nissila T. Self-assembly of binary solutions to complex structures. J Chem Phys. 2021;155(1):014904. doi: 10.1063/5.0053365
[312] Lutsko JF. Recent developments in classical density functional theory. In Rice SA, editor. Adv Chem Phys. Hoboken (NJ), USA: John Wiley & Sons, Inc; 2010. p. 1–92. doi: 10.1002/9780470564318.ch1
[313] Scacchi A, Nikkhah SJ, Sammalkorpi M, et al. Self-assembly in soft matter with multiple length scales. Phys Rev Res. 2021;3(2):L022008. doi: 10.1103/PhysRevResearch.3.L022008
[314] Archer AJ, Malijevsky A. Crystallization of soft matter under confinement at interfaces and in wedges. J Phys. 2016;28(24):244017. doi: 10.1088/0953-8984/28/24/244017
[315] Archer AJ, Rucklidge AM, Knobloch E. Quasicrystalline order and a crystal-liquid state in a soft-core fluid. Phys Rev Lett. 2013;111(16):165501. doi: 10.1103/PhysRevLett.111.165501
[316] Dhont JK. An introduction to dynamics of colloids. Amsterdam, Netherlands: Elsevier; 1996.
[317] Archer AJ, Evans R. Dynamical density functional theory and its application to spinodal decomposition. J Chem Phys. 2004;121(9):4246–4254. doi: 10.1063/1.1778374
[318] Reinhardt J, Brader JM. Dynamics of localized particles from density functional theory. Phys Rev E. 2012;85(1):011404. doi: 10.1103/PhysRevE.85.011404
[319] Rauscher M, Domínguez A, Krüger M, et al. A dynamic density functional theory for particles in a flowing solvent. J Chem Phys. 2007;127(24):244906. doi: 10.1063/1.2806094
[320] Aerov AA, Krüger M. Driven colloidal suspensions in confinement and density functional theory: microstructure and wall-slip. J Chem Phys. 2014;140(9):094701. doi: 10.1063/1.4866450
[321] Reinhardt J, Scacchi A, Brader JM. Microrheology close to an equilibrium phase transition. J Chem Phys. 2014;140(14):144901. doi: 10.1063/1.4870497

[322] Scacchi A, Archer AJ, Brader JM. Dynamical density functional theory analysis of the laning instability in sheared soft matter. Phys Rev E. 2017;96:062616. doi: 10.1103/PhysRevE.96.062616
[323] Scacchi A, Brader JM. Flow induced crystallisation of penetrable particles. J Phys. 2018;30(9):095102. doi: 10.1088/1361-648X/aaaa10
[324] Scacchi A, Mazza MG, Archer AJ. Sensitive dependence on molecular interactions of length scales in sheared soft matter. Phys Rev Res. 2020;2(3):032064. doi: 10.1103/PhysRevResearch.2.032064
[325] Archer AJ, Walters MC, Thiele U, et al. Solidification in soft-core fluids: disordered solids from fast solidification fronts. Phys Rev E. 2014;90(4):042404. doi: 10.1103/PhysRevE.90.042404
[326] Angioletti-Uberti S, Ballauff M, Dzubiella J. Dynamic density functional theory of protein adsorption on polymer-coated nanoparticles. Soft Matter. 2014;10(40):7932–7945. doi: 10.1039/C4SM01170H
[327] Tan H, Zhang M, Deng Y, et al. Sphere-forming diblock copolymers confined in a square well. Polymer. 2013;54(25):6853–6859. doi: 10.1016/j.polymer.2013.10.024
[328] Hao QH, Miao B, Song QG, et al. Phase behaviors of sphere-forming triblock copolymers confined in nanopores: a dynamic density functional theory study. Polymer. 2014;55(16):4281–4288. doi: 10.1016/j.polymer.2014.06.062
[329] Böbel A, Bott MC, Modest H, et al. Fluid demixing kinetics on spherical geometry: power spectrum and Minkowski functional analysis. New J Phys. 2019;21(1):013031. doi: 10.1088/1367-2630/aaf8d0
[330] Te Vrugt M, Löwen H, Wittkowski R. Classical dynamical density functional theory: from fundamentals to applications. Adv Phys. 2020;69(2):121–247. doi: 10.1080/00018732.2020.1854965
[331] Te Vrugt M, Wittkowski R. Perspective: New directions in dynamical density functional theory. J Phys. 2022;35:041501. doi: 10.1088/1361-648X/ac8633
[332] Brigham C. Biopolymers: biodegradable alternatives to traditional plastics. In: Green Chemistry. Amsterdam, Netherlands: Elsevier; 2018. p. 753–770. doi: 10.1016/B978-0-12-809270-5.00027-3
[333] Kumar A, Mishra RK, Verma K, et al. A comprehensive review of various biopolymer composites and their applications: From biocompatibility to self-healing. Mater Today Sustain. 2023;23:100431. doi: 10.1016/j.mtsust.2023.100431
[334] Ross CA, Poirier MA. Protein aggregation and neurodegenerative disease. Nature Med. 2004;10(Suppl 7):S10–7. doi: 10.1038/nm1066
[335] Elbaum-Garfinkle S. Matter over mind: liquid phase separation and neurodegeneration. J Biol Chem. 2019;294(18):7160–7168. doi: 10.1074/jbc.REV118.001188
[336] Bernaschi M, Melchionna S, Succi S. Mesoscopic simulations at the physics-chemistry-biology interface. Rev Mod Phys. 2019;91:025004. doi: 10.1103/RevModPhys.91.025004
[337] Shukla D, Hernández CX, Weber JK, et al. Markov state models provide insights into dynamic modulation of protein function. Acc Chem Res. 2015;48(2):414–422. doi: 10.1021/ar5002999
[338] Husic BE, Pande VS. Markov state models: from an art to a science. J Am Chem Soc. 2018;140(7):2386–2396. doi: 10.1021/jacs.7b12191
[339] Zeng QH, Yu AB, Lu GQ. Multiscale modeling and simulation of polymer nanocomposites. Progress Polym Sci. 2008;33(2):191–269. doi: 10.1016/j.progpolymsci.2007.09.002

[340] Deringer VL, Bartók AP, Bernstein N, et al. Gaussian process regression for materials and molecules. Chem Rev. 2021;121(16):10073–10141. doi: 10.1021/acs.chemrev.1c00022

[341] Hafner AE, Krausser J, Šarić A. Minimal coarse-grained models for molecular self-organisation in biology. Curr Opinion Struct Biol. 2019;58:43–52. doi: 10.1016/j.sbi.2019.05.018

[342] López Barreiro D, Yeo J, Tarakanova A, et al. Multiscale modeling of silk and silk-based biomaterials – a review. Macromol biosci. 2019;19(3):1800253. doi: 10.1002/mabi.201800253

[343] Rabotyagova OS, Cebe P, Kaplan DL. Protein-based block copolymers. Biomacromolecules. 2011;12(2):269–289. doi: 10.1021/bm100928x